Doctoral Dissertation

Development of transgenic *Daphnia magna* for visualizing homology-directed repair of DNA

Fatimah, Rizky Mutiara

May 2022

Biotechnology Global Human Resource Development Program,

Division of Advanced Science and Biotechnology,

Graduate School of Engineering,

Osaka University

Table of Contents

List of Figures

List of Tables

CHAPTER 1 GENERAL INTRODUCTION

1.1 DNA repair mechanism

Genomes are threatened by endogenously generated chemicals like reactive oxygen species and exogenous compounds such as mutagenic agents and radiation (Aguilera et al., 2008), which can lead to DNA double-strand breaks (DSBs). To ensure genetic stability and cellular viability, repairing the DSBs is essential.

The DNA repair mainly occurs through non-homologous end joining (NHEJ) and homology-directed repair (HDR) (Huertas, 2010). The NHEJ leads to ligation of the two ends of the DNA strand during which insertion or deletion of nucleotides (indels) can often occur at the cleavage site. The HDR repairs the DSBs by using information copied from undamaged DNA that has an identical or homologous sequence (homology) (Li et al, 2008). Many factors influence the pathway choice in DSB repair for instance cell cycle, the structure of DNA breaks, as well as chromatin, and nuclear position (Her et al, 2018).

The homology-directed repair system can be divided into four sub-pathways based on the mechanistic difference: double-strand break repair (DSBR), synthesis-dependent strand annealing (SDSA), break-induced replication (BIR), and single-strand annealing (SSA) (Huertas, 2010). First, in the DSBR, the formation of an intermediate structure with the Holliday junctions (HJs) leads to the generation of crossover and non-crossover products (Szostak et al., 1983). Second, the SDSA exclusively generates the non-crossover products due to the lack of formation of the HJ structure (Allers et al., 2001). Third, when only one ended DSB site has a sequence similar to that of the template, BIR occurs for non-reciprocal translocation of genetic information from the template strand (Morrow et al., 1997). Fourth, when the DSB is induced between the tandem repeats of the highly homologous regions, the SSA repairs the DNA by pairing the homologous region followed by deletion of unpaired DNA and the intervening region (F. L. Lin, et al., 1984). In the mitotically proliferating cells, the

SDSA is known to be the most common among the HDR sub-pathways (Andersen et al., 2010) which generates a non-crossover (NCO) product means that only the broken region was repaired and the template stays unaltered.

In the field of genome editing, the HDR also plays an important role due to its nature of high fidelity and accuracy. Unlike NHEJ considered to be error-prone, HDR avoids multiple integrations of donor DNA and indels between transgene and surrounding genomic region. Thus, precise genome modification can be achieved by utilizing programmable nuclease such as TALEN or CRISPR-Cas to introduce the DSB. For instance, the codon replacements or the seamless integration of the fluorescent reporter gene can be achieved by using donor DNA flanked with right and left locus-specific homology arms as a template (Yeh et al., 2019) (Bekker et al., 2018).

The HDR efficiency reported in mammals and plants is lower compared to NHEJ (Seluanov et al., 2010) (Mao et al., 2010) (Puchta, 2005). The HDR is more complex thus it takes a longer time to complete up to 7 hours than NHEJ which can be finished in 30 min (Mao et al., 2008). The HDR only occurs during S and G2 phases when the sister chromatid, the main template to repair DSB, is present (Pardo, et al., 2009). Hence, several approaches have been developed to enhance genome editing efficiency by HDR such as inhibiting (Chu et al., 2015) or knocking out the key factor of NHEJ (Nakanishi et al., 2015), synchronizing and capturing cells at certain phases (S. Lin et al., 2014), and modifying the Cas9 by fusing it with a key protein necessary in the HDR steps (Charpentier et al., 2018). To evaluate the effects of these approaches on the HDR activity, the reporter system for visualizing the HDR event has been used especially in mammalian cells (Pierce et al., 1999) (Słabicki et al., 2010).

1.2 the importance of HDR study especially in the *Daphnia magna*

The water flea *Daphnia magna* is a small freshwater crustacean found in broad continents such as Europe, the Middle East, Central Asia, Africa, and North America (Bekker et al., 2018).

The genus *Daphnia* reproduces by parthenogenesis under favorable environmental conditions but switches it to sexual reproduction in response to environmental stimuli such as shortened photoperiod, a lack of food, and/or increased population density (Herbert, 1978) as illustrated in Figure 1.

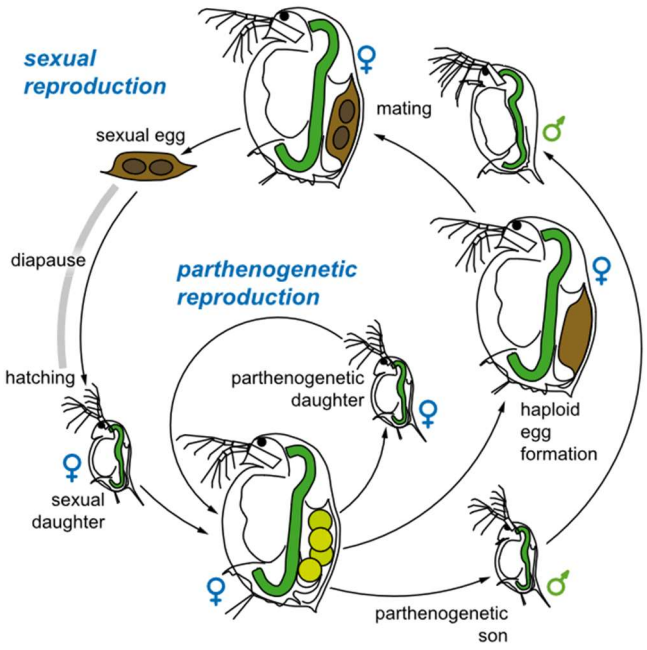

Figure 1. *Daphnia magna* life cycle.
In favorable conditions, the *D. magna* reproduce via a parthenogenetic life cycle resulting in a clone daughter. When the condition becomes harsh such as shortened photoperiod, lack of food or overpopulation the *D. magna* will enter sexual reproduction by producing male offspring and resting eggs. The resting egg is protected by an ephippium so that it can endure a harsh condition for a long period in a diapause state.
Picture source: https://commons.wikimedia.org/w/index.php?curid=47524211

The *Daphnia* genome contains at least 30,907 genes. This high gene count is resulted from duplication. By analyzing the frequency of pair-wise genetic divergence among all gene duplicates, it was reported that the gene duplication rate in *Daphnia* is three times higher than those measured in flies or nematodes, and 30% higher compared to humans. Among that, 20% of all genes were tandem gene clusters at the intervals of 1000-2000 bp (Colbourne et al., 2011). The tandem duplication clusters may serve as a template for HDR-based repair to attenuate the effect of deleterious mutations during the parthenogenetic cycle, which suggests that *Daphnia* may have a unique HDR mechanism.

D. magna occupies an important position in the freshwater food chain and is highly sensitive to chemicals. Thus, it makes this species a model in environmental and toxicological studies. The effects of several genotoxicants such as heavy metals (Arao et al., 2020) and human estrogen hormone (Törner et al., 2018) have been investigated at the phenotypic level. To further understand their actions at the molecular level which may affect the genome sequence, it is important to have a deep understanding of how the genotoxicants introduce the changes in DNA. One of the ways is by studying the DNA repair mechanism in this species in response to certain substances.

In the field of genome editing, the HDR-based knock-in of the exogenous DNA fragments has been reported in *D. magna* (Nakanishi et al., 2015) as well as the NHEJ-mediated knock-in (Kumagai et al, 2017), (Nakanishi et al., 2016). Comparing the efficiency, the HDR-based knock-in was low probably due to competition with the NHEJ pathway. To test this hypothesis, disruption of *DNA ligase IV,* the conserved component of the NHEJ pathway has been attempted (Nakanishi et al., 2015). However, its effect was not fully evaluated due to the lack of a method for quantifying the HDR event *in vivo*. Therefore, a system to evaluate and quantify the HDR event is a necessity.

1.3 Direct Repeat Green Fluorescence Protein (DR-GFP) reporter system

Fluorescence live imaging of the HDR event is essential not only for investigating how and where the genome integrity is maintained in living organisms but also for evaluating the HDR activity by manipulating the components for DNA repair. The direct repeat GFP (DR-GFP) reporter assay has been established for fluorescence-based visualization of the HDR activity (Pierce et al., 1999). The DR-GFP reporter system is composed of two mutated eGFP genes (Figure 2).

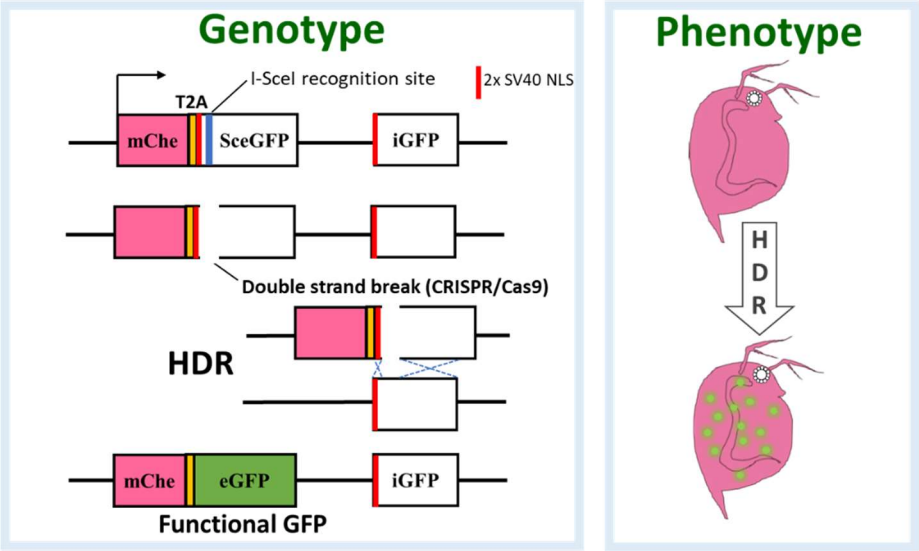

Figure 2. The DR-GFP reporter assay.
The DR-GFP reporter consists of two tandem repeats of mutated GFP. The first repeat (SceGFP, solid green) contains I-SceI recognition site with stop codons embedded (blue line). The second repeat (iGFP, striped-green) lacks 5′ and 3′ sequence. The introduction of DSB at the I-SceI site induces HDR-based DNA repair, utilizing homologous sequences from the iGFP, which in turn resulted in a functional eGFP gene (Genotype). The mCherry fluorescence will be ubiquitously expressed while the eGFP fluorescence signal will be observed in *D. magna* transgenic reporter as a result of the HDR event (Phenotype).

The upstream eGFP gene named *SceGFP* contains 18 bp of a recognition site of the rare-cutting I-SceI restriction enzyme. This recognition site contains two in-frame stop codons to terminate the protein expression. Downstream of the *SceGFP*, there is another mutated *eGFP* fragment termed internal GFP or *iGFP* which is an 812-bp internal GFP fragment. This reporter system visualizes the HDR event which is represented by its product. The functional GFP will be produced after HDR and can be detected by following the introduction of a double-strand break (DSB) with I-SceI restriction enzyme in the inactive *SceGFP* gene. The cleavage site will be repaired by HDR using *iGFP* fragment as the template.

Among the HDR sub-pathways, this DR-GFP system can visualize the non-crossover events that are mediated by the DSBR and SDSA (Paliwal et al., 2014) which is the majority of HDR sub-pathway in the meiotic and mitotic cell respectively (Andersen et al., 2010). This

suggests that the DR-GFP reporter can visualize the major HDR events spatiotemporally *in vivo*.

This reporter has been applied to study the factors that contribute to HDR in mice (Kass et al., 2013) and to study the role of a transcriptional repressor protein in HDR using *C. elegans* models (Johnson et al., 2013). However, the study of HDR in the crustacean is still lacking.

1.4 The objective of this study

Daphnia has a parthenogenetic life cycle in normal conditions (Herbert, 1978) moreover highly duplicated gene was found in its genome (Colbourne et al., 2011). It may suggest that it has a unique DNA repair pathway to neutralize the deleterious mutation that usually can be avoided by recombination during mating. In addition, in the case of genome editing, both NHEJ and HDR-mediated gene manipulation have been established in *D. magna.* However, the HDR-mediated technique still has low efficiency. Several attempts have been done to improve the HDR efficiency yet there is no system yet to evaluate the HDR event in *D. magna.* Hence, this study aims to establish the reporter transgenic *D. magna* which can visualize the event of HDR *in vivo*. First, I customized the DR-GFP reporter system which has been used to evaluate HDR levels in mammalian cells. I integrated the DR-GFP reporter into *D. magna* genome using CRISPR/Cas9 mediated knock-in. Lastly, I confirmed the functionality of the reporter system by introducing DSBs at the SceGFP region with the CRISPR/Cas9 system and detecting the eGFP signal spatiotemporally.

CHAPTER 2 GENERATION AND FUNCTIONAL ANALYSIS OF THE DR-GFP REPORTER TRANSGENIC *D. MAGNA*

2.1 Introduction

HDR as a DSB repair pathway that accommodates a precise correction is very important to cancel dangerous mutations. This repair pathway utilized the homolog sequences as a template to fix the DSB (Li & Heyer, 2008). The HDR frequency was lower compared to another main repair pathway, NHEJ. Because of its advantage to provide an accurate repair, several attempts to increase HDR efficiency (Chu et al., 2015) (Nakanishi et al., 2015) (S. Lin et al., 2014), (Charpentier et al., 2018). To improve the evaluation of HDR level, the utilization of a reporter system will be useful.

The system to evaluate the HDR could be utilized to study the mechanism of HDR in daphnia, study the genotoxicants' effect at the molecular level, and improve the HDR-based genome editing. However, the HDR reporter has not been reported in *D. magna*.

In this study, I aimed to generate the HDR reporter system in *D. magna* by adopting the DR-GFP reporter assay. By using the reporter HDR, evaluation of the DNA repair mechanism will be easier. I tried to customize the DR-GFP system that is originally utilized for mammalian cells (Pierce et al., 1999) so that it will be applicable for *D. magna*. Next, I integrated the DR-GFP system into *D. magna* genome utilizing the CRISPR/Cas9 system. By the knock-in via NHEJ-mediated genome editing that was previously established using Cas9 protein (Kumagai et al., 2017) a transgenic reporter was established. The functionality of the reporter transgenic was confirmed by introducing the DSB into an inactive eGFP fragment (SceGFP). The HDR event was evaluated by observing phenotype by the presence of eGFP fluorescence in the *D. magna* embryos as well the genotype by the detection of functional eGFP fragments in the genome using PCR.

2.2 Materials and Methods

2.2.1 *Daphnia* strains and culture conditions

Wild type *D. magna* (NIES clone) was obtained from the National Institute of Environmental Studies (NIES, Tsukuba, Japan) and has been maintained in the laboratory for many generations. The *D. magna* was cultured under the following conditions: 80 juveniles (less than 24 h old) were collected and cultured in 5 L Artificial Daphnia Medium (ADaM) that was prepared using reverse osmosis (RO) water as previously reported (Klüttgen, Dülmer, Engels, & Ratte, 1994). The temperature was set at 22-24^{o}C, under 16 h/8 h of light/dark photoperiod. *D. magna* were fed daily with 100 µL of 8 x 10^{9} cells of *Chlorella vulgaris* (Nikkai Center, Tokyo, Japan) and 15 µL of 0.15 g/mL baker's yeast (Marusan Pantry, Ehime, Japan) during the first week. Later, juveniles were removed daily and amounts of chlorella and yeast extract were doubled. The culture medium was changed once a week. For the later established DR-GFP transgenic line, the culture medium was changed twice a week.

2.2.2 Customization of donor plasmid

To construct donor plasmid pEF1α-1::mCherry-2A-DR-GFP, chicken β-actin promoter of pDRGFP from Addgene No.2647520 (Pierce et al., 1999) was replaced with *D. magna* EF1α-1 promoter. The fragment containing a complete sequence of EF1α-1 promoter was derived from the previously constructed plasmid (Kumagai et al., 2017). The two mutated eGFP fragments (SceGFP and iGFP) were amplified from the pDRGFP (Pierce et al., 1999). Lastly, for the integration into *D. magna* genome, a 200 bp sequence of *scarlet* gene harboring a gRNA target sequence (Izzatur et al., 2018) (Adhitama et al. 2018) was added. The fragments of the plasmid were amplified using KOD Plus DNA Polymerase (TOYOBO, Osaka, Japan). The sets of primers used in the reaction were listed in Table 1.

Table 1. List of primers for customizing the DR-GFP reporter plasmid.
The primers were synthesized by FASMAC (Tokyo, Japan).

Target region	Direction	Sequence (5′-3′)
pEF1α-1::mCherry-2A (Kumagai, Nakanishi, et al., 2017)	Forward	ACAAGTAAATGGAGGCTACTATTCCA
	Reverse	TTTTTTGGGGGCCCGGGATTTTC
SceGFP fragment (Pierce et al., 1999b)	Forward	CCGGGCCCCCAAAAAAGAAGAGAAAGG
	Reverse	AGAGTCGCGGCCGCTGTCCAAAT
pEF1α-1::mCherry-2A-SceGFP (this study)	Forward	AACTTCAACCCGGTACCCAGCTT
	Reverse	GGCTGCAGTAAGATACATTGATGAGTTTGG
iGFP fragment (Pierce et al., 1999b)	Forward	GTATCTTACTGCAGCCCAAGCTT
	Reverse	GTACCGGGTTGAAGTTCACCTTGATGC

All assemblies were performed using GeneArt Cloning & Assembly (Invitrogen, Carlsbad, USA). The constructed donor plasmid was purified using FastGene Plasmid Mini Kit (Nippon Genetics, Tokyo, Japan). The sequence of donor plasmid was confirmed by sequencing (Eurofins, Genomic, Japan). The donor plasmid used for microinjection was purified using PureYield Miniprep (Promega, Madison, USA) followed by phenol-chloroform purification, two times ethanol washing, and was re-suspended with Ultrapure water (Invitrogen).

2.2.3 In vitro transcription of guide RNA (gRNA)

The guide RNA (gRNA) targeting *scarlet* gene was synthesized using a cloning-free method from PCR-amplified template DNA as previously described (Gagnon et al., 2014). The sense synthetic oligonucleotide is 5′-**GAAATTAATACGACTCACTATAGG**TTCACTCGTCG CCTTAAT*GTTTTAGAGCTAGAAA*-3′. The sequence containing a T7 promoter sequence, a gene-specific target sequence, and the first 20 nt of the Cas9 binding scaffold are indicated with bold letters, underline, and italic letters respectively**.** The anti-sense synthetic

oligonucleotide is 5′-AAAAGCACCGACTCGGTGCCACTTTTTCAAGTTGATAACGGACTAGCCTTATTTTAACTT*GCTATTTCTAGCTCTAAAAC*-3′. It contains an 80 nt of Cas9 binding scaffold where the italic letter indicates the complement sequence with the sense oligonucleotides.

The template DNA was prepared by a PCR using the PrimeStar DNA Polymerase (TaKaRa, Shiga, Japan) with the following conditions: initial denaturation at 98ºC for 5 min; 15 cycles of denaturation at 98ºC for 10 sec, annealing at 55ºC for 30 sec, and elongation at 68ºC for 15 sec; lastly the elongation was held for 7 min. The PCR product was purified using MinElute PCR Purification kit (QIAGEN, Germantown, USA). gRNAs were synthesized using the MegaScript T7 Transcription Kit (Invitrogen), purified using Roche Mini Quick Spin RNA Column (Roche, Mannheim, Germany) followed by phenol/chloroform extraction, ethanol precipitation, and dissolved in UltraPure water (Invitrogen).

2.2.4 Generation of transgenic *D. magna*

For the generation of the DR-GFP line, the customized DR-GFP reporter plasmid was integrated into *D. magna* genome by utilizing the CRISPR/Cas-mediated knock-in via non-homologous end-joining as previously reported (Kumagai et al., 2017). Microinjection into *D. magna* embryos was performed following an established protocol using the *S. pyrogenes*-originated Cas9 proteins (Kato et al., 2012) (Kumagai et al., 2017). The Cas9 proteins were expressed in *E. coli* strain BL21 (DE3) and purified following established protocol (Honda et al., 2017). Fifty nanograms per microliter of purified donor plasmid were co-injected with 2 μM *scarlet* targeting gRNA, 1 μM Cas9 protein, and 2 mM Lucifer Yellow fluorescence dye (Thermo Fisher Scientific, MA, USA). Shortly before the microinjection, Cas9 protein and gRNA were incubated at 37ºC for 5 minutes to form a ribonucleoprotein (RNP) complex. The needle for injection was made of 0.6 mm ID glass capillary (Narishige, Tokyo, Japan). The glass was pulled using a capillary puller machine (Sutter Instrument, Novato, USA). The tip of

the needle was cut using an insect pin (Shiga, Tokyo, Japan). The injection solution was loaded to the needle using Microloader (Eppendorf, Hamburg, Germany). The amount of injection solution was confirmed by checking the volume at approximately 0.2 nL in Mineral Oil Nuclease and Protease tested (Nacalai Tesque, Kyoto, Japan) droplet after pressing the pedal for 3-5 sec. The nitrogen gas as the pressure source was set at 250-500 kPA and the balance pressure was set at 18 kPA to avoid contamination of injection solution. Microinjection was performed within two hours after the preparation of the solution to maintain the quality of the RNP complex. After injection, the intact eggs were transferred, cultured individually in a sterile 96 well plate, and put in an incubator at 22 ºC with 16 h/8 h of light/dark photoperiod for 3 days. Each well of the 96 well-plate (BD Falcon, USA) was filled with 100 µL of M4-sucrose.

2.2.5 Screening for G0 candidates and genotyping

Transgenic candidates were screened based on the mCherry expression in the ovary of injected embryos (G0). The G0 was observed using the mCherry filter (Leica Microsystem) on Leica M165FC fluorescence microscope (Leica Microsystem, Wetzlar, Germany). The mCherry expressing G0s were cultured and genotyping was performed using the second generation offsprings (G2).

For the genotyping, the transgenic candidates were collected and homogenized in 500 µL lysis buffer (50 mM Tris-HCl pH 7.5, 20 mM EDTA pH 8.0, 100 mM NaCl, 1% SDS) using MicroSmash homogenizer (TOMY, Tokyo, Japan) at 3000 rpm for 1.5 min with the presence of 0.15 mg/mL Proteinase K (Nacalai). The homogenized daphniids (lysate) were shaken overnight at 55ºC, 450 rpm using an incubator shaker (Bioshaker M-BR-022UP, TAITEC, Tokyo, Japan). To obtain genomic DNA (gDNA), the lysate was purified using phenol/chloroform extraction, precipitated with isopropanol, rinsed twice with 80% and 70% ethanol, and dissolved in 50 µL TE buffer before being used as a template for genomic PCR.

The PCR was performed by using an Ex Taq Hot-Start DNA polymerase (TaKaRa) with primer sets amplifying the target region as described in Table 2.

Table 2. List of primers for genotyping the DR-GFP transgenic candidates.
The primers were synthesized by FASMAC (Tokyo, Japan).

Target region	Direction	Sequence
mCherry	Forward	5′-GGCCATCATCAAGGAGTTC-3′
	Reverse	5′-CGTTGTGGGAGGTGATGTC-3′
5′ junction region of integration site	Forward	5′-TGGAGACGTCATTCGATTACG-3′
	Reverse	5′-CTGGCGTAATAGCGAAGAGG-3′
3′ junction region of integration site	Forward	5′-CAGCCATACCACATTTGTAG-3′
	Reverse	5′- GTTGAGCGACTGGTATCTTC -3′
Scarlet 2nd allele	Forward	5′-TTCCATTGCTCATACAACC-3′
	Reverse	5′-GCAAAGTAGATTTCCCTGC-3′
Beta-actin	Forward	5′-GGCAAGGAATAGTTCGATAC-3′
	Reverse	5′-CACCGACGTACGAATCCTTCTGACC-3′

The PCR was performed using Takara Thermal Cycler PCR machine with the following conditions: initial denaturation at 98 ºC for 5 min; 30 cycles of denaturation at 98 ºC for 10 sec, annealing at 55 ºC for 30 sec, and elongation at 68 ºC for 1 min; next the elongation was held for 5 min. The PCR product size was confirmed by agarose gel electrophoresis.

2.2.6 Functional analysis of DR-GFP reporter transgenic *D. magna*

To check the functionality of the DR-GFP reporter system in *D. magna,* I attempted to introduce the DSB at 2 bp upstream of the I-SceI digestion site that was previously used for I-SceI-dependent DSBs (Pierce et al., 1999). Therefore, using Benchling

(https://www.benchling.com/benchling-molecular-biology) the guide RNA (gRNA) was designed to recognize the 18bp of I-SceI site as shown in Figure 3.

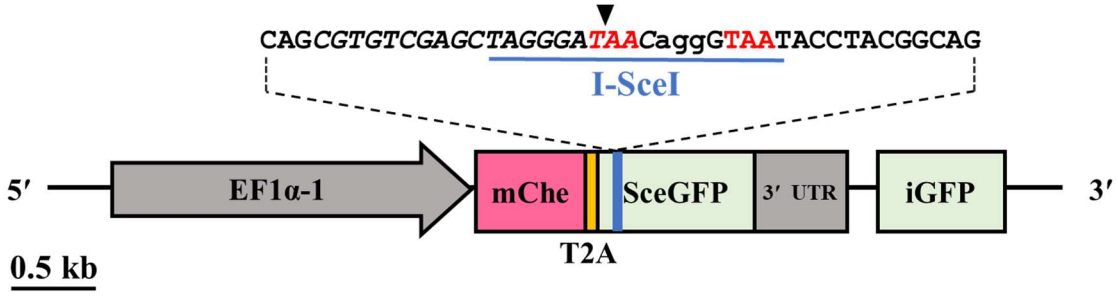

Figure 3 The DR-GFP The SceGFP gRNA target site

SceGFP contains a recognition site of the 18 bp I-SceI restriction enzyme and in-frame two stop codons indicated in the blue underline and red letter respectively. SceI gRNA was designed to correspond with the I-SceI recognition site (italic) upstream of the PAM sequence (small letter). The cleavage site of SceI gRNA was indicated by a black triangle.

To confirm whether Cas9 was active during microinjection, we also co-injected the SceI gRNA with another gRNA targeting *Distal-less (Dll)* gene. Previously RNAi-mediated knockdown of *Dll* in embryos of *D. magna* led to a distinct phenotype "truncation of second antennae" and the level of this truncation corresponded to the degree of impairment of this gene (Kato et al., 2011). The Dll gRNA was designed to target the upstream of the homeodomain region in exon 2 as shown in Figure 4.

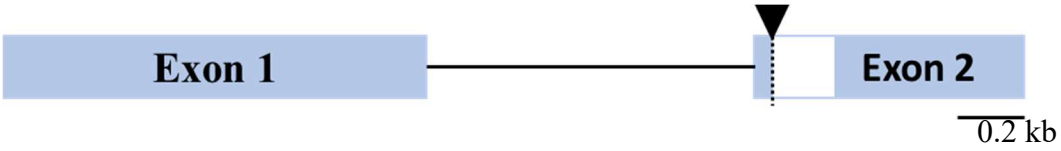

Figure 4. Distal-less (Dll) gRNA location

Illustration of exons 1 and 2 of *Dll* gene in *D. magna*. gRNA target (dash line) is located upstream of the homeodomain region (white box) of *Dll* gene.

The homeodomain is highly conserved among arthropods (Kato et al., 2011) and is considered important for Dll protein function because it contains a sequence-specific DNA binding site as part of a transcriptional regulator (McGinnis et al., 1992). Another report suggested it is required for the elaboration of proximodistal pattern elements in limbs

development (Panganiban et al., 2002). The phenotypes of the second antennae of the injected embryos were observed 48 hours post-injection (hpi) and categorized as normal, mild, medium, or strong truncation (Figure 5) (Kato et al., 2011).

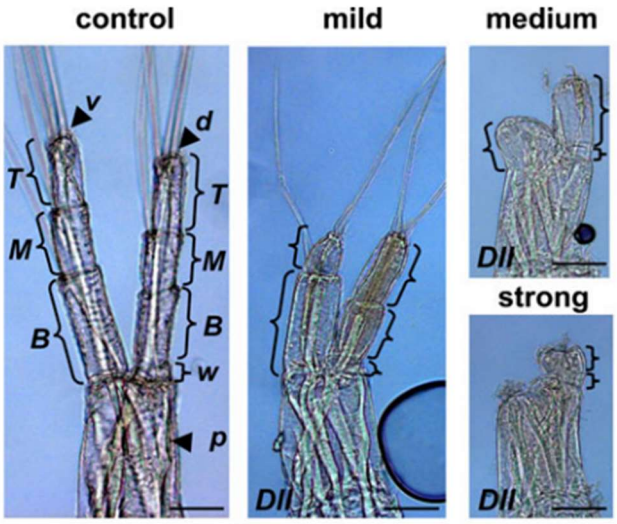

Figure 5. Classification of the second antenna phenotype.
In normal phenotype, second antennae consist of a protopodite (*P*), carrying a dorsal and ventral ramus. Each ramus has three segments, Terminal (*T*), Middle (*M*), and Basal (*B*). There is an additional small wedge-shaped segment (*w*) between *B* and *P*. Mild truncation exhibit, a part of *M* and full *B* (ventral ramus), full *M*, *B*, and *w* (dorsal ramus). Medium truncation: a trace of *B* (ventral), *B,* and *w* (dorsal). Strong truncation: only a trace of *B* and *w* (dorsal) (Kato et al., 2011).

Guide RNAs (gRNAs) were synthesized using a cloning-free method from PCR-amplified template DNA as previously described in section **2.2.3** (In vitro transcription of guide RNA (gRNA)). The sense synthetic oligonucleotide containing a T7 promoter sequence, a gene-specific target sequence, and the first 20 nt of the Cas9 binding scaffold are shown in Table 3.

Table 3. The sense sequence of the oligonucleotide for SceI and Distal-less gRNA synthesis
A T7 promoter, a targeting sequence, and the first 20 bp of the Cas9 binding scaffold sequence were indicated with bold letters, underline, and italic letters respectively.

No	gRNA Target	Sense oligonucleotide

1	SceI	5′-**GAAATTAATACGACTCACTATA** **GG**TGTCGAGCTAGGGATAAC*GTTTTAGAGCTAGAA*-3′
2	Distal-less (Dll)	5′-**GAAATTAATACGACTCACTATA** **G**CAAGAAGATGCGCAAACCG*GTTTTAGAGCTAGAA*-3′

The co-injection of 1 µM Cas9 protein and gRNA mixtures (SceI gRNA and Dll gRNA, 2 µM each) was performed in the established transgenic line. 5 µM AlexaFluor 568 fluorescent dye (Invitrogen, Carlsbad, USA) was used as a control for injection volume. The microinjection protocol is the same as mentioned before in section **2.2.4** (Generation of transgenic *D. magna*).

2.2.7 Fluorescence photography

The samples were observed and photographed at 48 hpi (hour post-injection) using the Leica DC500 CCD Digital Camera mounted on the Leica M165FC fluorescence microscope (Leica Microsystem, Wetzlar, Germany). 48 hpi was chosen as at this time point, the phenotype of the second antenna could be observed. The mCherry filter (Leica Microsystem) and the GFP3 filter (Leica Microsystem) were used to observe repaired SceGFP after the HDR. The parameter for the photography was shown in Table 4.

Table 4. Parameters for the observation

Filter	**Bright Field**	**GFP**	**mCherry**
Exposure time	4.0 ms	8.0 s	1.0 s
Gain	4.0 x	4.0 x	4.0 x
Saturation	1.0	1.2	1.2
Gamma	0.5	1.0	1.0

2.2.8 Genotyping for detecting the product of HDR event

To confirm whether HDR occurred at the genomic level, the uninjected embryos and injected embryos that showed nuclear-localized eGFP fluorescence were subjected to a genomic PCR. The genome DNA (gDNA) of the embryos was extracted by using the simplified phenol/chloroform method as previously described in section **2.2.5** (Screening for G0 candidate and genotyping). The primer set was designed in the *mCherry* region for the forward primer and recognizes specifically the sequence of the repaired *SceGFP* for the reverse primer as shown in Figure 6.

A.

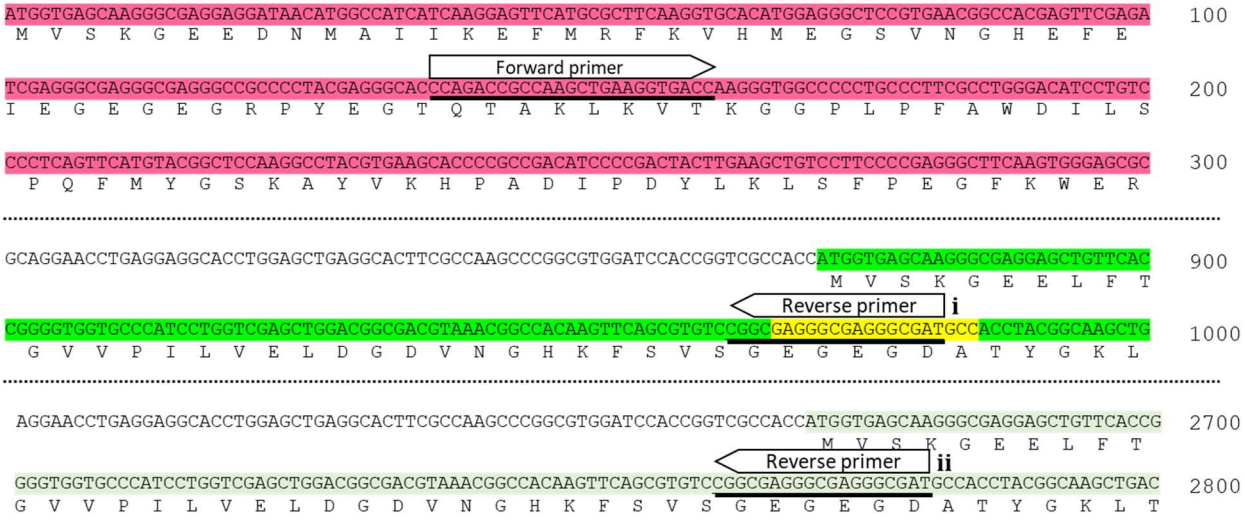

B.

SceGFP : 5′-CGGCTAGGGATAACAGGGTAATACCTACGGCAA-3′

Repaired SceGFP : 5′-CGGCGAGGGCGAGGGCGATGCCACCTACGGCAA-3′

Figure 6. The genotype of DR-GFP transgenic after DSB introduction

(A) PCR was performed on uninjected and injected DR-GFP genome using primer pairs indicated by arrows. The forward primer is attached in the mCherry region (pink area) while the reverse primers are attached in two locations, the repaired *SceGFP* (yellow area) and *iGFP* (light green). **(B)** Alignment between *SceGFP* and repaired *SceGFP* or *eGFP*. The reverse primer was designed to bind specifically to the repaired *SceGFP* (underline).

The PCR was performed using Ex Taq Hot-Start DNA polymerase (TaKaRa) with the following conditions: initial denaturation at 98 ºC for 5 min; 30 cycles of denaturation at 98 ºC for 10 sec, and extension at 72ºC for 1 min; next the extension was held for 5 min. The PCR product size was confirmed by 1% agarose gel electrophoresis.

2.2.9 In vitro transcription and microinjection of Cas9 mRNA

I attempted to develop a qPCR-based that can detect the repaired SceGFP expression. As a model to test this system, Cas9-mRNA and Cas9 protein were used for introducing the DSB on the *SceGFP* because mutagenesis efficiency with Cas9 mRNA was lower than that with Cas9 protein (Kumagai et al., 2017), which suggested Cas9 mRNA induces DSB occurrence to a lesser extent.

For Cas9 mRNA synthesis, a template DNA containing T7 promoter sequence was PCR amplified from pCS-Dmavas-Cas9 (Nakanishi et al., 2014). Capped mRNA synthesis and poly(A) tail addition were performed using mMessage mMachine T7 kit and Poly(A) Tailing Kit (Invitrogen) respectively. Synthesized mRNA was column purified by using Roche Mini Quick Spin RNA Column (Roche) followed by phenol/chloroform extraction, ethanol precipitation, and lastly dissolved in UltraPure water (Invitrogen). mRNA integrity and the addition of poly(A) tails were confirmed by denaturing formaldehyde gel electrophoresis.

The DSB was introduced at the *SceGFP* by co-injecting 500 ng/µL Cas9 mRNA and 50 ng/µL SceGFP gRNA which is the optimum condition of Cas9 mRNA in the *D. magna* (Nakanishi et al., 2014). The 50 ng/µL of Dll gRNA was co-injected to evaluate the Cas9 activity in each injection. 250 ng/µL of GFP mRNA was co-injected as the control for mRNA degradation during the injection.

2.2.10 Total RNA extraction

Injected and uninjected embryos were collected at 48 h post-injection. The total RNA was extracted in the presence of Sepasol-RNA I solution (Nacalai Tesque) according to the

manufacturer's protocol. The total RNA was purified using phenol/chloroform extraction, precipitated with 70% ethanol, dissolved in UltraPure water (Invitrogen), and directly subjected to reverse transcriptase reaction.

2.2.11 RT-qPCR

To detect repaired *SceGFP* mRNA level, qPCR was performed in StepOnePlus (Applied Biosystem) using KOD SYBR® qPCR Mix (Toyobo, Osaka, Japan) with primers as listed in Table 5.

Table 5. List of primers for qPCR reactions

The primers were synthesized by FASMAC (Tokyo, Japan).

Target region	Direction	Sequence
Repaired SceGFP	Forward	5′-TTCTAACATGCGGGGACGTG-3′
	Reverse	5′-CAGCTTGCCGTAGGTGGCAT-3′
mCherry	Forward	5′-CTACGACGCTGAGGTCAAGAC-3′
	Reverse	5′-GGTGTAGTCCTCGTTGTGGG-3′
L32	Forward	5′-GACCAAAGGGTATTGACAACAGA-3′
	Reverse	5′-CCAACTTTTGGCATAAGGTACTG-3′

cDNAs were synthesized from 1 μg of purified total RNA using random primers and PrimeScript II 1st strand cDNA Synthesis Kit (TaKaRa). The *β-actin* gene was amplified by PCR to confirm the absence of genomic DNA contamination as previously described (Kato et al., 2018).

The cycling condition is as follows: 2 min at 98 ºC, followed by a total of 40 cycles of 98 ºC for 10 s, 60 ºC for 10 s, and 68 ºC for 30 s. Primers' specificity was confirmed by melting curve analysis and agarose gel electrophoresis. The expression level of Repaired *eGFP* was normalized using that of *mCherry* which is controlled under the same promoter.

2.3 Result

2.3.1 Customization of donor plasmid

To visualize the HDR by fluorescence in *D. magna*, a previously established DR-GFP reporter plasmid (Pierce et al., 1999) was customized as shown in Figure 7.

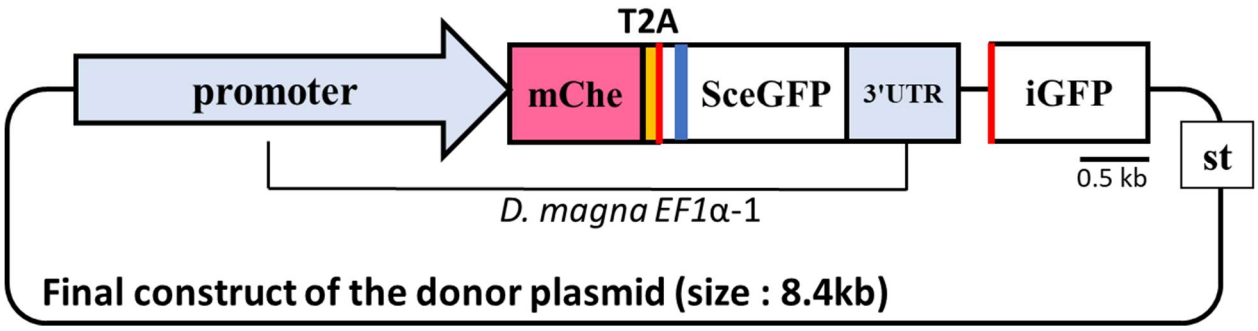

Figure 7. The donor plasmid design
The direct repeat of differentially mutated *eGFP* (DR-GFP) consists of mutated (*SceGFP*) and 5′ and 3′-lacking sequence of *eGFP* (*iGFP*), both are indicated in light green boxes. Three repeats (two complete and one partial) of the simian virus 40 large T-antigen nuclear localization signal (SV40 NLS) are included in the *SceGFP* sequence. The reporter system is expressed ubiquitously under *D. magna EF1α-1* promoter/enhancer (grey arrow). The red fluorescence protein mCherry-coding sequence is placed upstream of the DR-GFP system. *mCherry* and DR-GFP are bicistronically expressed using *Thosea asigna* virus 2A (T2A) peptide indicated in the yellow box. *SceGFP* contains a recognition site of the 18 bp I-SceI restriction enzyme and in-frame two stop codons indicated in the blue line.

A red fluorescent protein gene mCherry ORF was fused upstream of the SceGFP via a sequence encoding *Thosea asigna* virus 2A (T2A), which can lead to bicistronic expression of both mCherry and mutated/repaired eGFP proteins (Kumagai et al., 2017). To distinguish the eGFP-expressing cells individually, the three nuclear localization signals (two complete and one partial) of the simian virus 40 large T-antigen nuclear localization signal (SV40 NLS) were included in the SceGFP (Donoho et al., 1998).

To express the DR-GFP reporter, a 2.3 kb of *D. magna* EF1α-1 genomic fragment including the promoter/enhancer, the transcription start site, the complete first intron, and part of the second exon with a start codon was used (Kato et al., 2012) (Kumagai et al., 2017). In

addition, to recapitulate EF1α-1 endogenous expression, the full-length EF1 α-1 3′ UTR was added downstream of the reporter. This DR-GFP reporter will function when the DSB is introduced in the I-SceI site by the Cas9-gRNA complex.

2.3.2 Generation of DR-GFP reporter *D. magna*

To integrate the customized DR-GFP reporter into *D. magna* genome, the CRISPR/Cas-mediated knock-in via non-homologous end-joining was used (Kumagai et al., 2017). As a target site for knock-in of the reporter plasmid, I chose exon 3 of the eye pigment transporter *scarlet* gene (Izzatur et al., 2018). The co-injection of DR-GFP reporter plasmid and the RNP complex into 213 eggs was performed. The 105 injected embryos survived until adult stage, from which 78 adults have the white eye that is the typical phenotype of the *scarlet* mutant (Table 6).

Table 6. Injection summary of knock-in experiment to generate the reporter transgenic

Injection batch	Embryos	Juvenile	Adult	K.O.	K.I.	
					Somatic	Germline
1	29	10	10	9	0	1
2	19	12	11	9	0	0
3	41	21	16	14	0	0
4	45	21	19	10	0	0
5	29	19	19	14	1	0
6	50	40	30	22	1	0
Total	**213**	**123**	**105**	**78 (74%)**	**2 (2%)**	**1 (1%)**

This phenotype indicates that the Cas9 RNP induced DSBs at the targeted site. Of the 78, three had ubiquitous mCherry fluorescence, and one adult passed the phenotype to its offspring, suggesting germline transmission of the reporter plasmid. The mCherry fluorescence

pattern also indicates that this reporter system enables us to detect the HDR event in most types of cells (Figure 8).

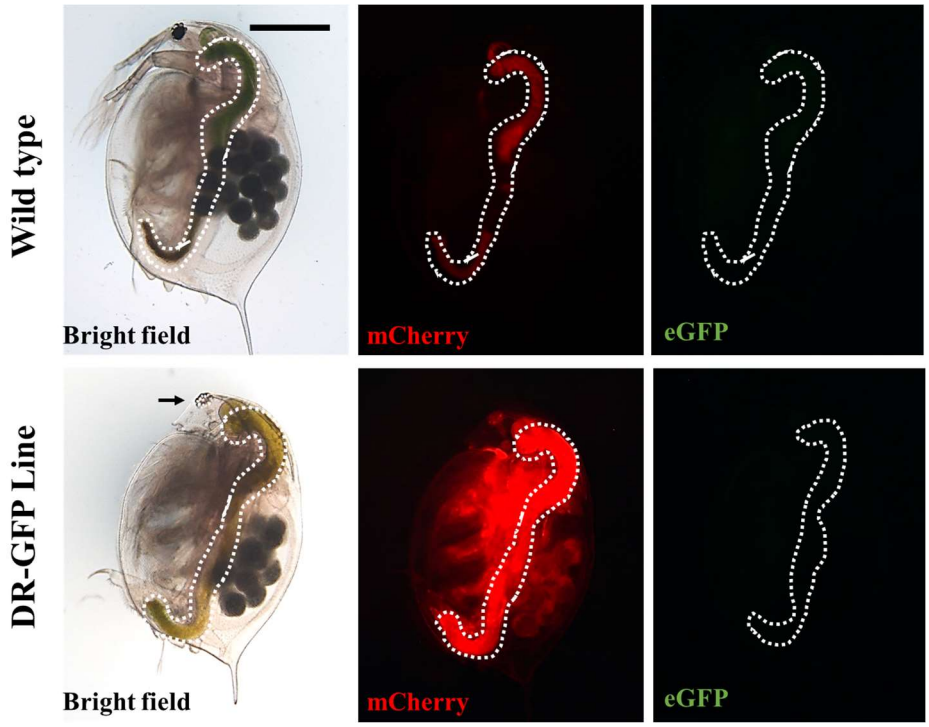

Figure 8. The phenotype of the DR-GFP line

Comparing phenotypes of the DR-GFP line with the wild-type *Daphnia*. The top and lower rows show *D. magna* obtained from wild type and DR-GFP lines respectively. The image in each column was photographed using either of bright field, mCherry, or GFP3 filter. The region inside the white-dashed line is the gut, in which ingested chlorella emits slight red autofluorescence both in wild type and DR-GFP. Widespread mCherry fluorescence was observed only in the transgenic line, while eGFP fluorescence was not observed. Black arrow indicates loss of black eye pigment due to disrupted *scarlet* allele. The scale bar indicates 1 mm.

This potentially transgenic line was cultured until it produced second-generation (G2). To investigate whether NHEJ-mediated knock-in occurred, genotyping was performed using the genome of the potentially transgenic line G2. I amplified the mCherry fragment, 5′ and 3′ junctions between the transgene and its surrounding region by PCR. The illustration is shown in Figure 9.

A.

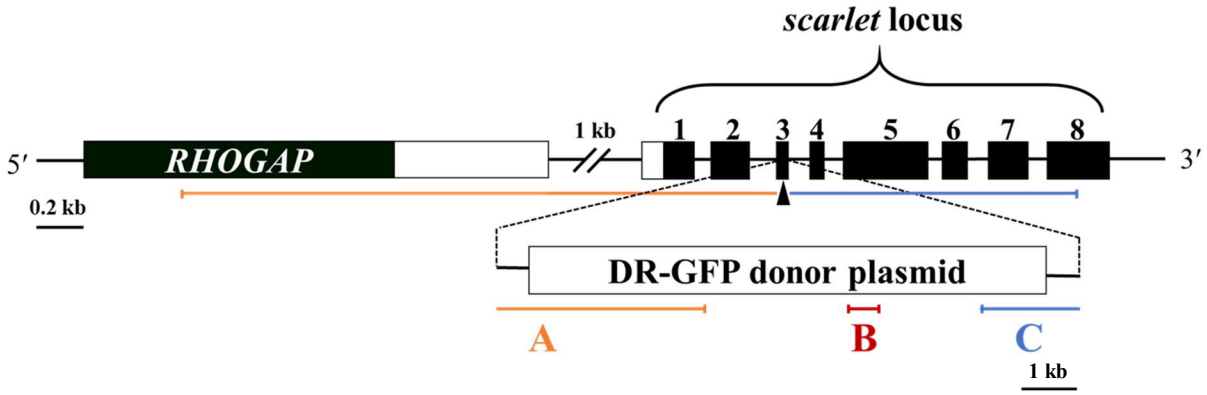

B.

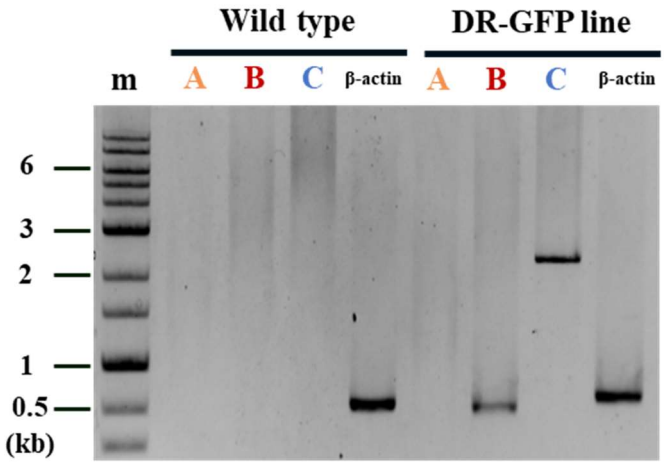

Figure 9. The genotype of the DR-GFP line

(A) Schematic representation of the integration site of the DR-GFP donor plasmid. A part of *RHOGAP* (Rho-GTPase activating protein) gene is shown upstream of *scarlet*. The DR-GFP donor plasmid was integrated into exon 3 of the *scarlet* gene. A and C indicate the 5′ and 3′ junction regions of the donor plasmid and genome, B indicated the internal region of the donor plasmid (*mCherry* gene). **(B)** PCR result was visualized by gel electrophoresis. The first lane is the marker, followed by fragments A, B, C, and β-actin (beta-actin) for both wild type and DR-GFP line *Daphnia*. In the sample using DR-GFP line *Daphnia,* all fragments except the 5′ junctions were amplified.

The expected size of the mCherry fragments was obtained only in the potential transgenic line (Figure 9B, fragment B, DR-GFP line). The 3′ junction region was also amplified in this line by using forward primer targeted at the downstream of EF1 α -1 3′ UTR of the donor plasmid and reverse primer targeted exon 8 of scarlet gene locus (Figure 9A;

Figure 9B, fragment C, DR-GFP line). Sequencing of this PCR product confirmed the integration of the reporter plasmid at the scarlet locus and revealed 20 bp deletion and 8 bp insertion at the 3′ side of the integrated cassette (Figure 10, 3′ junction). Consistent with the white-eyed phenotype, another allele contained indel mutation at the DSB site (Figure 10, 2nd allele).

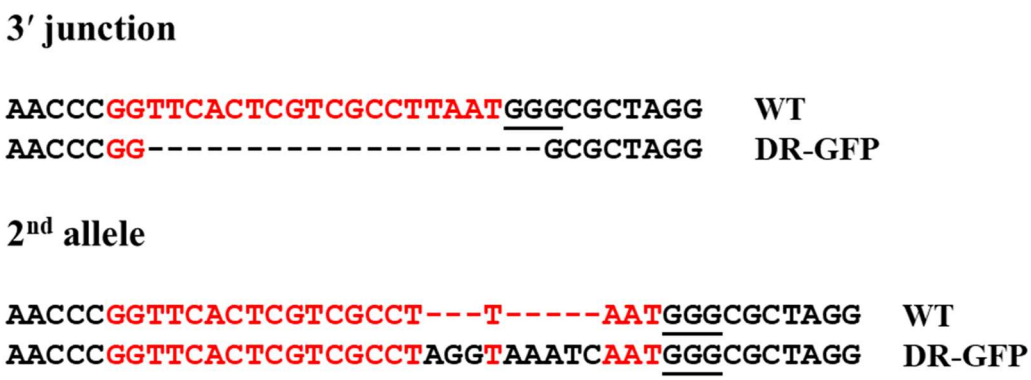

Figure 10. Deletion in the 3′ junction region and second allele of the scarlet locus

20 bp deletion and 8 bp insertion were detected in the 3′ junction of plasmid integration and another allele of *scarlet* respectively. The red-colored nucleotides and black triangle indicated the St gRNA target and DSB site respectively

The 5′ junction region was unable to be amplified even if the forward primer was designed at 3,157 bp upstream and 2,610 bp downstream of the DSB site (Figure 9, fragment A). This suggests that large deletion occurred at the 5′ side of the integration site.

ef1α1 promoter/enhancer region

mCherry coding region

HA tag region

T2A region

SV40 NLS region

Zinc finger DBD of GAGA transcription factor

SceGFP region

TaqI recognition site

I-SceI recognition site

ef1α1 3' UTR region

iGFP region

Scarlet target site region

scarlet gRNA spacer sequence

indel mutation region

scarlet gene exon region

*every line represents 100 bp nucleotide

5'-

cgccagtcggagcaagcttgatttaggtgacacAGCTTCAGCGACCTTGGGGAAAATTTTCAACTCACACAGCTATTGATTAAATTTAAAGGTAACGTTG

CTTTTATCGCCTTGTTTCAAATTGTAGCCAGTTACACCCTGGGCCGTTCCTTTCAGTCATTTGGTAAGATTGATCGACAATCGTGGAGCTGTGCCCTTCC

TTTATACTGGGAAAACAATGCAATACTTACAAGATGTAGAGTGGCTTATAGTTACATAGAACATCTCTGGCTTGTAAATATTTACACTAAGTAATTGTCA

TTTCATACAGGAAGTGATGTAAGGAGCAATACAACGACTATTGAGAAATTTATTGGTTGTTTTCTAGAAATACATGCGTGATCACCACATTGCTCGTTGA

ACTCCAGACAGTTTGTTGTAATCGGCCAAGCTACGCCAAACAATTCGACTCAATCTCCAGCGCGTGACGACGCCTCTTGGACGGGACGTGATGGCACAGC

GATTGCGTACGCGGGTTAAGCTCGCATCTCGAGGAATTTCAGCTAGCATTTTGGTACCAATCTCCTTCAAACAAAATCTTTAAATGAGGGGTTCTTAAAC

TTGTTGTATACTTTAAAGAATATACTGATGCTTATCCTATGATTGCATGAATTGATCTTAATATTTTAAAAAATTTATATAAAAATTCAACAACAGTGCA

AACCCAACGCAACAAAATTAATGAAAAAATAGTGTGAAATCCCATGCAAAACTTGTTAAAGCTCGATATTGGGTAAATAACTTAATAGGCCTGTGAGAGA

ATTAGTTCAACTAAGAATGAAGGGTAGTTCTAAATTACTATTATCTCAGCAGGCAAAACATCATTTTTTTTTAGGGCTTTTGCGCGAACACGGTCAGGTG

CGTATTGGACGAGTAATTTTCGTCGCCGGTTATCCTTCATCATTCTCCAATCTGTCCAATTGTTTCTGACTGGTTGATTCAATTTTACTGCATTTGTCAT

CTAAGAAATTTTGTTTTGTTTACGTAACTGATATATAAAACGAAAAATATAAAAACATACTCCATTTCGAAGTAGTTGGGCGGTGTTTTGCAATAAAAAA

CTTGAAAAATTTAACAATTTGCTCATGGTAGTCGTGATGGCCATTTTGTTCTGAAGAGTAAACAAAGAGATGTCAAATCGACAAATCAGACTTGCAAGAA

AACATTTTCAAACAACGTTAAACTTTATAGTTGTTAAGATAAAAATTTTAAAATCAAAAATTCATTTGGGAACAATGTGTTTTTTTTTTTTTACCTTGAA

AACAACCTTGTGCAAAGCCCCTAGAGAGGGGGAGAAATATCCGAGGGAGAAAAAAATTTAAATAACCTTGAAAGAAGCATCAGTAAATAGATTGTGGTTG

TTTGATAAAATCAAAAATTAATAATCTACATTTTTCTAACATTAATCAATTGAAATGTTATAAAATTAAACAATGTTTAACGCAATGCAACTCTGTTCCC

CTCCCCTGTAGAGACTTTACTCCGTAGGGGCTAGCAACTTCCAGCGTCACTCGTTCTCGTGTCTTTCAAGGTTCGTTCTCTTCTCTTCCAACGGAACATC

AGGTAAGCACACGTTTTGACGCGTCTCCCAAATTTATCCTCGCAAATCGAAGTATTCTTTGTCAATCCATTAGTAACAATGTCTTCAAAGCATAGAAATA

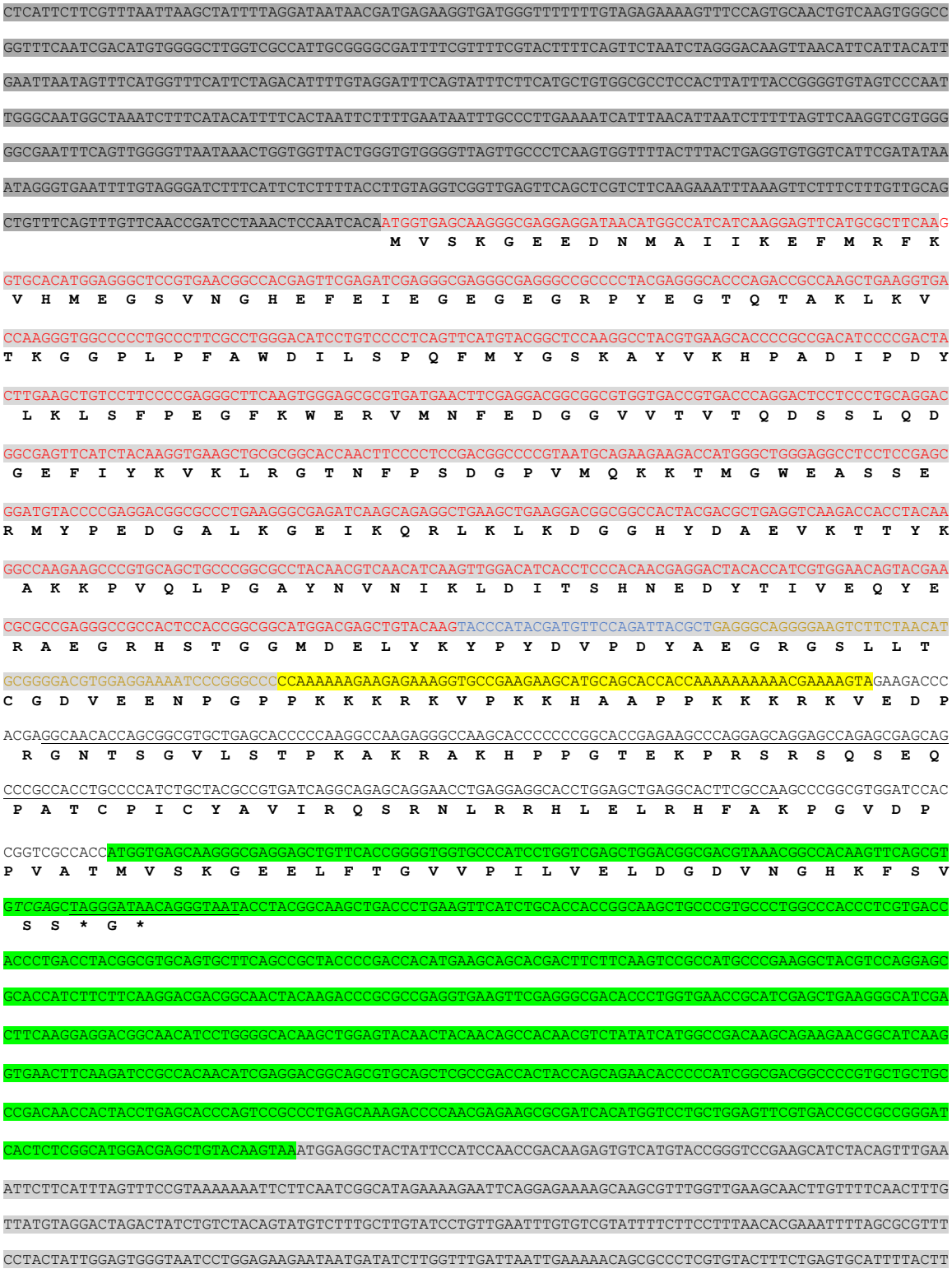

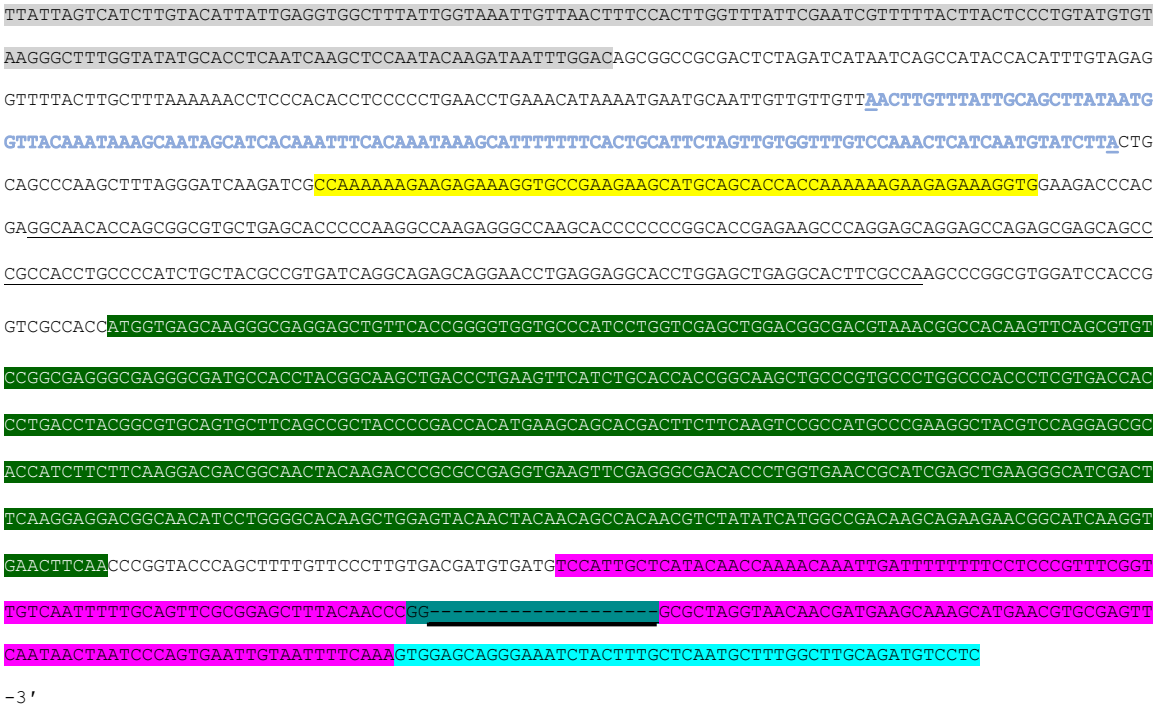

Figure 11. The full sequence of the integrated DR-GFP reporter in the *D. magna* genome

Nevertheless, amplification and sequencing of the full-length of the DR-GFP gene cassette demonstrated the integration of the intact DR-GFP reporter (Figure 11). This knock-in daphniid was named the DR-GFP line

.

2.3.3 The DSB near the I-SceI site leads to the generation of eGFP-positive cells in embryos of the DR-GFP line

To confirm the efficiency of Dll-gRNA, i*n vivo* assay was performed by injecting the Dll-gRNA and Cas9 protein into wild type *D. magna* with three different volumes. 48h post-injection, the phenotype of truncated antennae was observed. The results showed that 100% of developed embryos had truncated antennae (Figure 12).

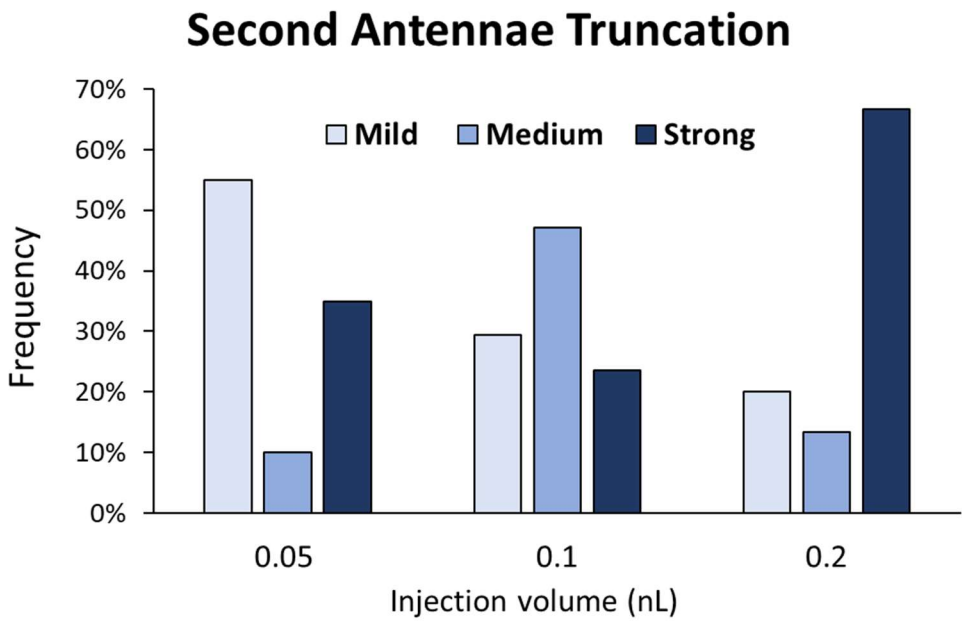

Figure 12. The Cas9 activity corresponded to the second antennae phenotype.

Level of second antennae truncation corresponded to the injection volume. As shown in Figure 12 the lowest volume resulted in mild truncation as the majority while the highest volume had a strong truncated phenotype as the majority. Therefore, it was concluded that Dll gRNA co-injection could be used as an internal control for Cas9 activity.

After confirming the Dll gRNA efficiency, forty-three embryos survived until the 48 hpi stage and 41 (95%) showed truncation of the second antennae (Table 8) from which, 22 embryos (54%) showed strong phenotype (Kato et al., 2011), indicating that Cas9 was active during injection and could introduce DSBs on the genome.

Table 7. Summary of Cas9 protein, SceI gRNA, and Dll gRNA co-injection

Injected	Developed	Truncated antennae	Nuclear-localized eGFP

	(48hpi)	Strong	Medium	Mild	
74	43	22/41 **(54%)**	9/41 **(22%)**	10/41 **(24%)**	33/41 **(80%)**

Of the 41, 33 (80%) showed strong nuclear-localized eGFP fluorescence in the tissues such as the head and thoracic appendages. (Figure 13). In contrast, embryos injected with Cas9 RNP including the unrelated *St* gRNA (Figure 13) and Dll gRNA did not show intense and nuclear-localized GFP signal, indicating that the recovery of the eGFP fluorescence occurred by injection of Cas9 protein and SceI gRNA. The remaining 8 samples did not show any eGFP signal. Probably due to the three-dimensional structure of *D. magna,* eGFP positive cells located deep inside the tissue were hard to be detected.

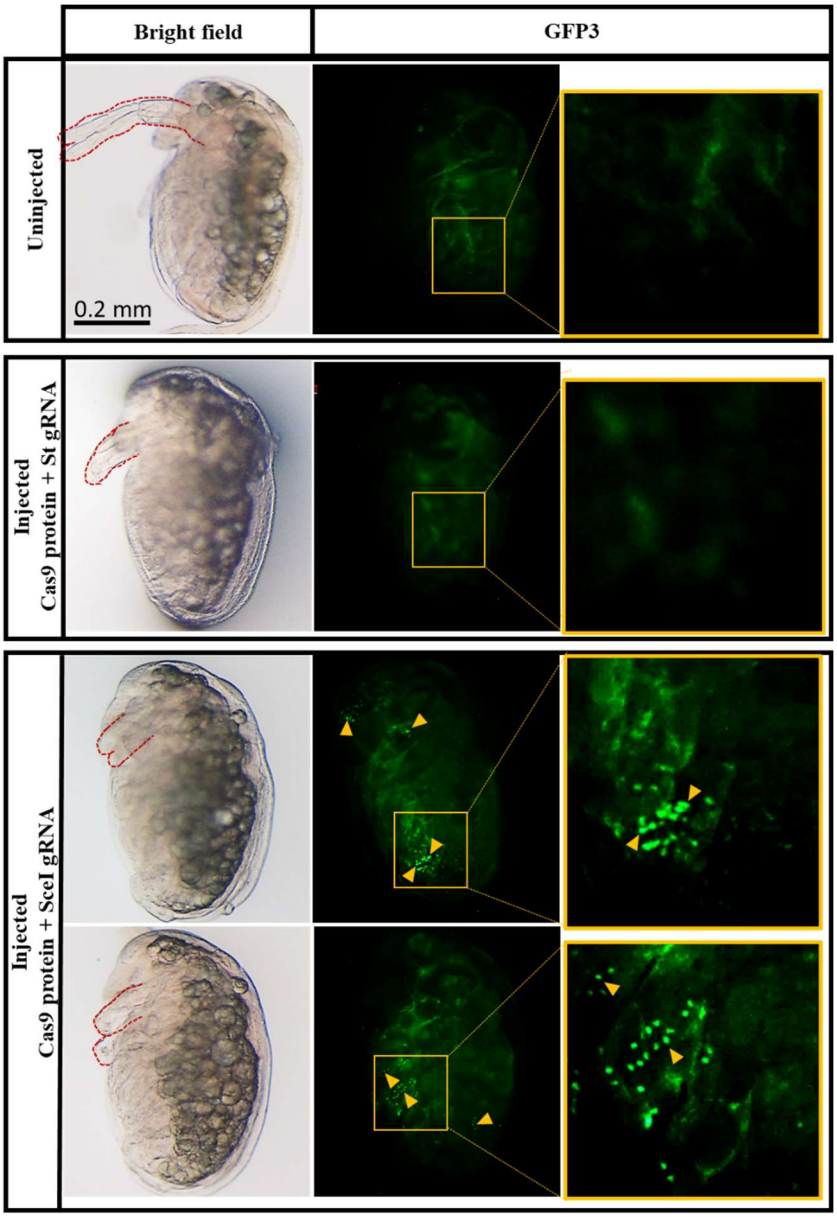

Figure 13. Detection of eGFP-positive cells of DR-GFP transgenic D. magna following the DSB in the SceGFP

DR-GFP line was co-injected with Cas9 protein, SceI gRNA, and Dll gRNA. The injection of Cas9 protein with St gRNA and Dll gRNA was performed as a control. The first row shows uninjected control, while the second, third, and fourth rows show injected individually *Daphnia*. Images were taken using the bright field and the GFP3 filter. All daphniids were photographed at 48 h post-injection. The red dashed line shows the second antennae region, which was truncated because of Dll gRNA injection. The weak background green fluorescence observed throughout the body of all samples was coming from autofluorescence. The repaired *SceGFP* was controlled under *EF1α-1* promoter/enhancer and contains NLS, resulting in abundantly expressed and nuclear-localized eGFP expression (yellow triangles).

To confirm whether HDR occurred at the genomic level, the genome DNA from uninjected embryos and injected embryos that showed nuclear-localized eGFP fluorescence

was extracted. PCR was then performed with a forward primer in the mCherry region and a reverse primer that recognizes specifically the sequence of the repaired SceGFP (Figure 14). Because the reverse primer also can bind to the iGFP sequence that is a template for HDR, two bands were expected to appear upon genomic PCR (Figure 14, i and ii).

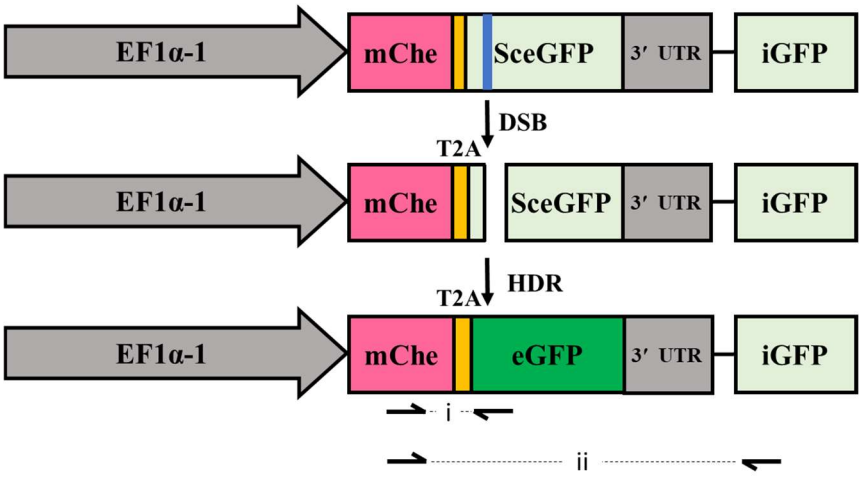

Figure 14. The primer position for genotyping the DR-GFP transgenic after DSB introduction

PCR was performed on uninjected and injected DR-GFP genome using primer pairs indicated by arrows. The forward primer is attached in the mCherry region (pink) while the reverse primers are attached in two locations, the repaired *SceGFP* or *eGFP* (green box) and *iGFP* (light green).

The gel electrophoresis result shows a higher size band (2,843 bp) was present in all samples, indicating amplification from iGFP sequence (Figure 15, ii), while a lower size band (1,048 bp) indicating amplification from repaired SceGFP sequence was obtained only from embryos injected with Cas9 and SceI gRNA (Figure 15, i). These results also suggest the repair of SceGFP by Cas9 and SceI gRNA.

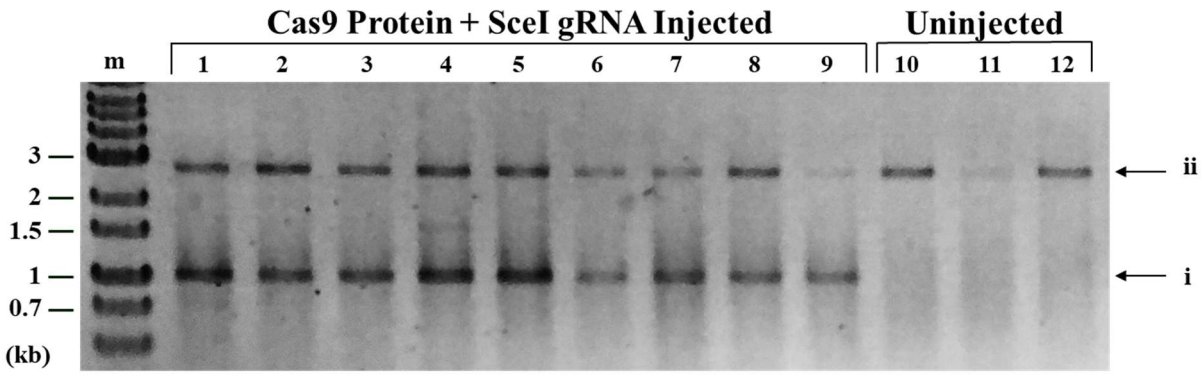

Figure 15. Gel electrophoresis result

The most left lane indicated the DNA marker (m) followed by amplified genome fragments (lanes 1-9) from Cas9 Protein and SceI gRNA injected embryos. Uninjected DR-GFP (lanes 10-12) was used as the negative control. The primer set amplified the repaired *SceGFP* region with the length of 1,048 bp (i). The reverse primer was also attached to the *iGFP* region, which resulted in a 2,843 bp length PCR product (ii)

By integration of DR-GFP reporter into *D. magna* genome and confirmation of the DR-GFP reporter functionality, it was concluded that the fluorescence-based live imaging of HDR in *D. magna* was achieved. This established transgenic line could provide a spatiotemporal HDR event *in vivo*.

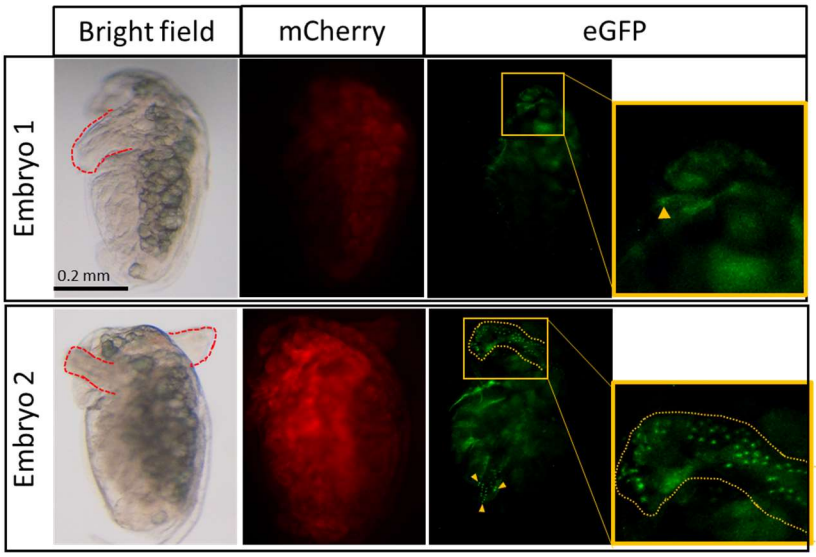

Figure 16. The variation in the DR-GFP reporter expression.

The different mCherry fluorescence intensity between two embryos. Embryo 1 (upper figure) which had mCherry fluoresce compared to Embryo 2 (lower figure) also had a smaller number of eGFP-positive cells.

However, several limitations of this system were found. First, there was a variation in the reporter expression level. It was detected by the individual difference of mCherry intensity

since it was driven by the same promoter as the DR-GFP reporter cassette. As shown in Figure 16, the embryo with darker mCherry also showed a lower number of eGFP-positive cells. Some embryos might not have a detectable eGFP signal due to the low expression of the DR-GFP reporter

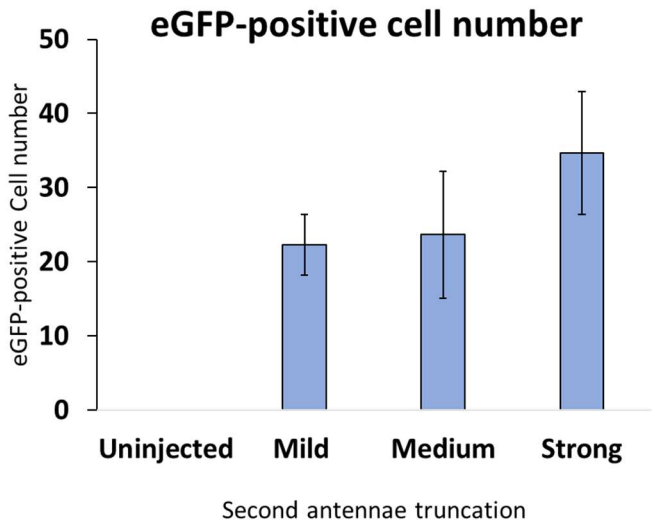

Figure 17. The number of eGFP-positive cells in different degrees of the second antennae truncation.
The eGFP-positive cells resulted from HDR event between mild, medium, and strong second antennae phenotype of injected samples. (Mild, N=10; Medium, N = 9; Strong, N=22).

The Cas9 activity could be represented by the second antennae truncation degree by the Dll gRNA co-injection. It was suggested that the stronger activity of Cas9 to produce DSB, the more HDR event could be detected by the presence of eGFP signal. Thus, the number of GFP-positive cells was counted to see the correlation with the second antennae truncation. From a total of 41 injected embryos that showed truncated antennae, the embryos were classified based on the phenotype of the second antennae truncation. The number of eGFP-positive cells showed a positive correlation with the second antenna truncation (Figure 17) where the mild truncation had the lowest number of cells and samples with strong phenotype have the highest number of eGFP-positive cells. However, it was statistically no significant difference due to a

big individual difference among the samples, and also some cells deep inside the tissue might not be observed under the microscope.

2.3.4 qPCR-based method could detect the repaired SceGFP as the product of HDR event

To improve the detection of eGFP-positive cells by microscope and also to standardize the expression level among the samples, I attempted to develop a qPCR-based method that can detect the repaired SceGFP expression. A forward primer that binds to the T2A-coding sequence of DR-GFP reporter locus and a reverse primer that specifically binds to repaired *SceGFP* sequence (Figure 18) were designed. In the genome, the reverse primer also could bind with the iGFP fragment because it was used as a template during HDR repair. To avoid the background signal coming from the PCR product which is the amplicon from iGFP fragment, the mRNA was used instead of genomic DNA for qPCR analysis. The iGFP fragment will not be amplified because it is lack of downstream region responsible for the polyA signaling process. Moreover, driven by EF1α-1 promoter the mRNA was continuously expressed resulting in more copy numbers than genomic DNA. It could enhance the detection of a low level of repaired SceGFP in the genome.

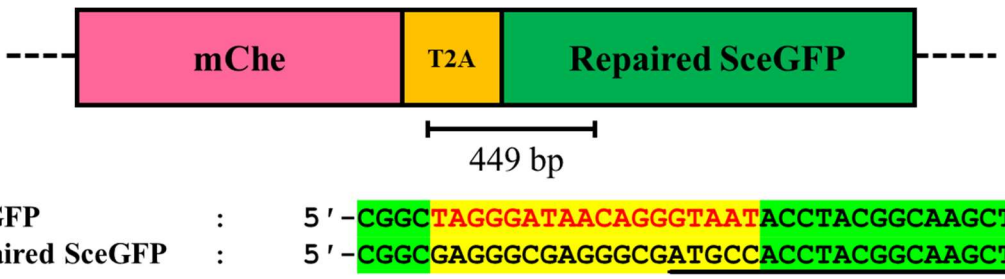

Figure 18. Detection of the functional eGFP transcript by qPCR
(A) The position of primers and the region used for quantifying the repaired *SceGFP* level (above) were shown in the black line. **(B)** The alignment showed that the reverse primer was designed to specifically bind to repaired *SceGFP* fragment (underline).

Cas9-mRNA and Cas9 protein injection for introducing the DSB on the *SceGFP* was used as the model for this system. The previous report implied that mutagenesis efficiency with

Cas9 mRNA was lower than that with Cas9 protein (Kumagai et al., 2017), which suggested that Cas9 mRNA induces DSB occurrence with lower efficiency. I confirmed 54% of Cas9 protein injected embryos showed a strong phenotype of second antennae truncation while Cas9 mRNA could only introduce a mild phenotype (Table 7 and Table 8 for Cas9 protein and mRNA respectively).

Table 8. Summary of Cas9 mRNA, SceI gRNA, and Dll gRNA co-injection

Injected	Developed (48hpi)	Truncated antennae			Nuclear-localized eGFP
		Strong	Medium	Mild	
24	10	0	0	8/8 **(100%)**	**Not observed***

*To confirm the integrity of the Cas9 mRNA, the eGFP mRNA was also co-injected for confirmation of the mRNA integrity based on the eGFP fluorescence intensity. This prevented us from observing the nuclear-localized eGFP signals in the Cas9 mRNA-injected embryos.

This result implied that Cas9 protein had stronger activity to introduce DSB consistent with previously reported (Kumagai et al., 2017). In the mRNA injected samples, the nuclear-localized eGFP signal from the HDR event could not be observed because the eGFP mRNA was co-injected as a control for mRNA integrity during microinjection. Hence, the high background of eGFP signal coming from injected eGFP mRNA prevented us to observed the nuclear-localized eGFP as the product of repaired SceGFP by HDR. Subsequently, the level of repaired *SceGFP* was analyzed using qPCR. The result shows by Cas9 protein injection, a significantly higher expression of repaired *SceGFP* (~5 fold) relative to Cas9 mRNA injection was observed (Figure 19)

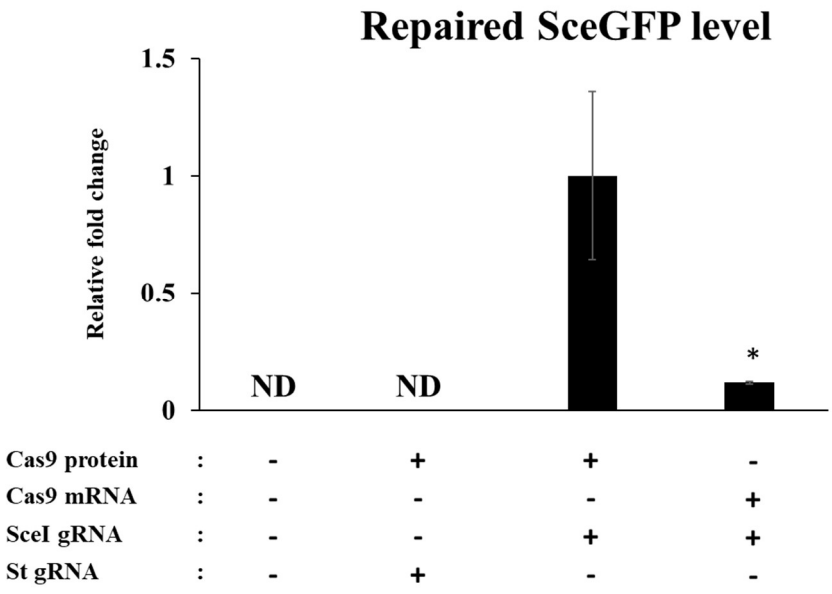

Figure 19. eGFP transcript between injected samples

Level of repaired *SceGFP* between injected and uninjected samples after the introduction of DSB. The value was quantified by qPCR. There was a significant difference between Cas9 protein and mRNA injection. The values are means and error bars represent standard error (N=3). * $p<0.05$ (Student's *t*-test). In uninjected embryos and ones injected with Cas9 protein and scarlet gRNA, the repaired SceGFP mRNA was not detected (ND).

Moreover, neither repaired *SceGFP* signal nor amplification was detected in uninjected embryos as well as scarlet gRNA injected embryos (Figure 20). This result shows that qPCR can be used to detect the functional eGFP repaired by HDR. Previously reported that the qPCR could detect at least 3 molecules at 95% confidence (Forootan et al., 2017). It suggested that the number of repaired SceGFP cDNA molecules presented in the uninjected and scarlet gRNA injected embryos was less than 3. However, the detection limit is also affected by noise from the sample handling and analysis process.

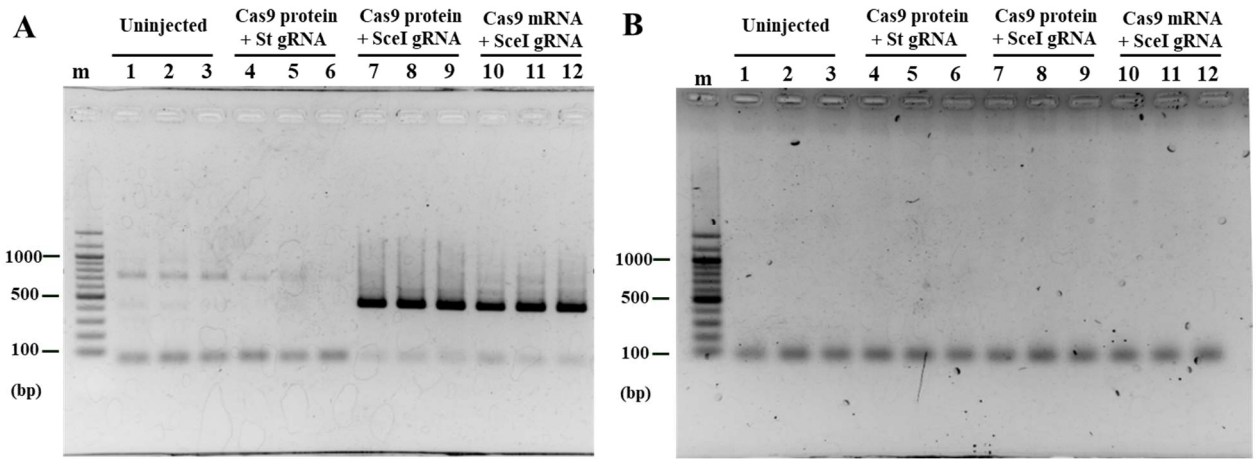

Figure 20. Gel electrophoresis of the qPCR result

(A) The first lane is the marker (m). Repaired *SceGFP* PCR product which was expected to be 449 bp was only observed in the Cas9 protein (lane 8-10) and mRNA (lane 10-12) co-injection with SceI gRNA. **(B)** The DNA marker was put in the first lane. All of the samples (lane 2-13) showed a band that was expected to be 67 bp indicating the PCR product of L32 as an endogenous gene for control of cDNA template.

2.4 Discussion

I reported the generation of transgenic *D magna* which can visualize the HDR in vivo by integration of DR-GFP reporter into its genome. The DR-GFP reporter was widely utilized to study the pathway of HDR such as revealing the roles of HDR key factors during DNA repair in mammalian cells (Pierce et al., 1999b) (Stark et al., 2004) (Bunting et al., 2010) as well as the whole organism (Kass et al., 2013) (Johnson et al., 2013). To apply this system in *D.magna* customization is needed to make the reporter applicable to our model organism. The original donor plasmid harboring the DR-GFP from Addgene No.2647520 (Pierce et al., 1999) contains chicken β-actin promoter. This promoter was replaced by *D. magna* EF1α-1 promoter to allow ubiquitous expression of the reporter (Kato et al., 2012) (Kumagai et al., 2017) together with the addition of EF1α-1 3`UTR.

To ease the screening for transgenic candidates, I utilized two different markers. The marker for knock-out was the *scarlet* gene which is chosen as the integration site. The introduction of mutation in the *scarlet* locus enables us to screen the transgenic candidates for

the lacking of eye pigment resulting in a white-eye phenotype. The mutants lacking *scarlet* function were confirmed to have equal fitness (fecundity) with the wildtype (Izzatur et al., 2018). The genome integration marker was the *mCherry* ORF which was fused upstream of the SceGFP separated by T2A peptide that can lead to bicistronic expression in *D. magna* as previously reported (Kumagai, Matsuura, et al., 2017). The viral 2A peptide that contains 19 amino acid sequences can mediate the protein cleavage allowing the production of two different proteins from one single mRNA (Ryan, King, & Thomas, 1991). Once the DR-GFP reporter was integrated into the genome, a strong mCherry fluorescence under EF1 α-1 was observed. Furthermore, the *puromycin-resistant* gene that was previously used for cell screening in the original pDR-GFP (Pierce et al., 1999) was removed from the donor plasmid to reduce the size of the donor plasmid. As a previous study suggested that the shorter insert resulted in higher integration efficiency (Paix et al., 2017).

The established transgenic reporter, the DR-GP line, has a white eye as the typical *scarlet* knock-out phenotype. The genotyping and sequencing result on the *scarlet* locus revealed that 8 bp insertion was introduced resulting in the frameshift and premature stop codon. As one allele has the integration of DR-GFP reporter it makes the DR-GFP line has no functional *scarlet* gene in both alleles. In addition, it has an mCherry fluorescence in the whole body while the eGFP expression was not observed. This phenotype indicates that the DR-GFP reporter system which is placed under the same promoter as mCherry is expressed in most types of cells in the *D. magna* body.

The functionality of the reporter system was confirmed by introducing the DSB near I-Sce site. Following the HDR pathway, DSB ends in the SceGFP region are recognized by nucleases and subjected to 5′ end resection resulting in 3′-OH single-stranded tails. The tails associated with Rad51 protein search and invade the DNA region which has high sequence homology as the template (Li et al., 2008), in this reporter system is iGFP region. After DNA

synthesis, the invading strand is dissociated and reannealed with the second end (Li et al., 2008) resulting in a new fragment of repaired SceGFP which is a functional *eGFP* gene. The observation of 48 embryos post-injection suggested the functional eGFP could be observed by its dotted-like characterization. Moreover, the genomic PCR result clearly showed that the repaired SceGFP fragment, as a result of HDR event, was only present in the injected samples. Altogether, these suggested that the DR-GFP *D. magna* could detect the HDR event in vivo.

The microscope observation is limited to 2D observation. The cell inside the daphnia body may not be detected. To improve the sensitivity of the detection, I attempted to utilize qPCR method the monitor the HDR event. By using cDNA as the template for qPCR, the transcript of repaired SceGFP fragment could be detected. The result showed that Cas9 protein had stronger activity to introduce DSB. This result is consistent with previously reported (Kumagai et al., 2017) and suggested that the qPCR-based method could be used to detect the product of HDR events.

The limit of detection defines the sensitivity of this reporter system. Ideally, the HR reporter should be able to detect even 1 occurrence of an HDR event in a single cell. While qPCR analysis may detect as low as one copy of HDR-repaired gene, the detection limit of the DR-GFP reporter system itself should be characterized. In the future, such a limit could be determined by exposing the DR-GFP line to different doses of stimuli (i.e. nuclease or genotoxicants). After observing the nuclear-localized eGFP under the microscope, the samples could be analyzed by qPCR by using genome DNA as the template. A standard curve correlating the CT value and copy number of the repaired SceGFP shall be made and thus limit of detection could be determined.

CHAPTER 3 GENERAL DISCUSSION AND CONCLUSION

3.1 General Discussion

D. magna has an important position as a primary consumer in the freshwater food chain moreover, it is also highly sensitive to chemicals. These traits make *D. magna* for ecotoxicology. So, it will be beneficial if we could have a system which to monitor the effect of genotoxicant at the molecular level. In addition, *D. magna* has a parthenogenetic life cycle which will always produce female offspring in favorable conditions. This might be a disadvantage because without recombination via mating, mutation accumulation might occur and resulted in unwanted mutation. However, a previous study revealed that *Daphnia* genome contains highly duplicated genes (Colbourne et al., 2011). Those gene clusters may serve as a template for HDR-based repair to cancel the deleterious mutation. So, it will be useful to have a system that could visualize the HDR event in *D. magna.* Moreover, in terms of genome editing, the utilization of HDR could be applied to introduce error-free genome editing to avoid disruption in the proximal target sites. The low efficiency of HDR might be caused by the competition with the NHEJ pathway. To test the hypothesis, the system to evaluate the HDR event is essential.

In this study, I aimed to establish a reporter system that can visualize HDR events in *D. magna*. I integrated the DR-GFP reporter system in *D. magna* genome (Figure 21, genotype). I confirmed its functionality by introducing DSBs at the *SceGFP* region with the CRISPR/Cas9 system and detecting the eGFP signal spatiotemporally (Figure 21, phenotype). Furthermore, I could detect the repaired eGFP gene by genomic PCR and qPCR, which adds merit to this system to be utilized for the evaluation of the HDR event. By applying different stimuli (Figure 21, stimuli), the established transgenic *Daphnia* might contribute to various scientific fields such as ecotoxicology, genome editing, and evolutionary biology.

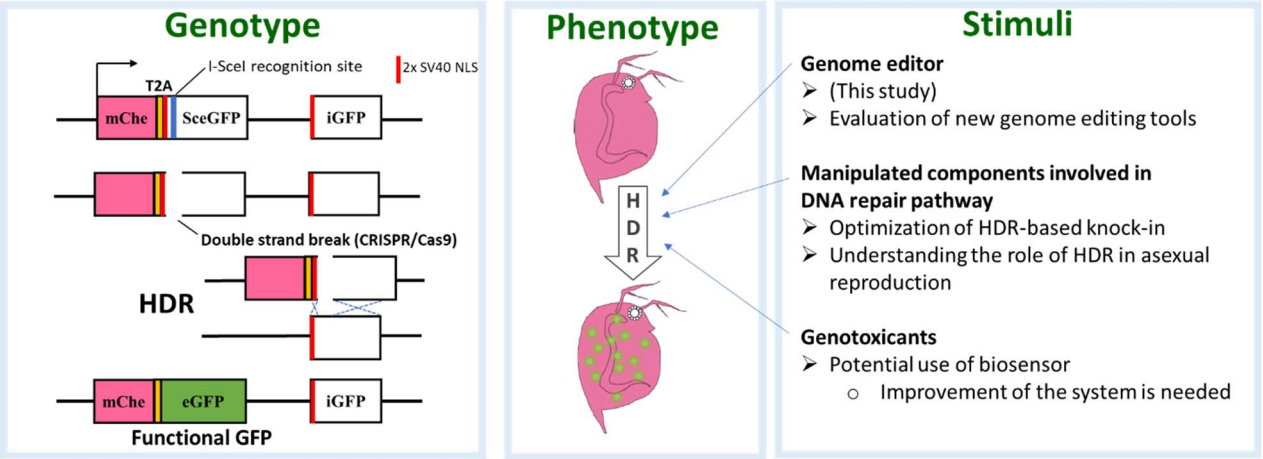

Figure 21. The DR-GFP reporter assay and its potential application
The DR-GFP reporter system is integrated into the *D. magna* genome (left box figure). The eGFP fluorescence signal will be observed in *D. magna* transgenic reporter as a result of the HDR event (middlebox figure). The possible application of the transgenic reporter is to elucidate the effect of various stimuli on the HDR level (right box).

I used the DR-GFP line to compare Cas9 mRNA and Cas9 protein ability to introduce DSB and induce HDR in *D. magna*. By using qPCR, we detected significantly higher repaired *SceGFP* expression in the Cas9 protein injected samples (Figure 19). This result was in line with a difference in DSB-inducing activity between Cas9 protein and mRNA in *D. magna* (Kumagai et al., 2017). Recently, genome editing techniques using the CRISPR/Cas system are rapidly developing with the emergence of novel and smaller Cas9 proteins, such as *Staphylococcus aureus* derived Cas9 (SaCas9) (Ran et al., 2015) and synthetic RNA-guided nuclease (sRGN, surgeons) (Schmidt et al., 2021). As the DR-GFP system was also used to measure HDR DSB and single-strand break (SSB)-inducing activity using Cas9 and Cas9 nickase respectively in HEK293T cells, we anticipate our DR-GFP *Daphnia* could be a promising tool for the evaluation of new genome editing tools (Figure 21, genome editors).

The DR-GFP system also has been applied for the screening of genotoxicants such as heavy metals (Deininger et al., 2016), FDA-approved drugs for cancer therapy (Shahar et al., 2014) in addition to evaluation of the sensitivity of the cancer cell to gamma-ray irradiation

(Osaki et al., 2016). The aquatic ecosystem is constantly exposed to genotoxicants, and *D. magna* has been long used as a workhorse for ecotoxicology analysis as a biosensor. The test guideline for acute or chronic toxicity test for *Daphnia* is well established by following the OECD Guideline (OECD, 2004), (OECD, 2012). The DR-GFP *Daphnia* may be suitable for screening genotoxicants in vivo (Figure 21, genotoxicants).

In recent years, several transgenic animals containing the DR-GFP system have already been established for analyzing the molecular mechanisms of HDR. For instance the generation of DR-GFP reporter mouse for analyzing the HDR frequencies in primary cell types derived from diverse lineages (Kass et al., 2013). In *C. elegans* (Johnson et al., 2013), the DR-GFP system was integrated into the genome to identify a novel role of protein in promoting HDR. *Daphnia* might have a unique DNA repair mechanism to neutralize the genetic drawbacks because its asexual ability might lead to the accumulation of deleterious mutations due to the absence of recombination events via mating. I anticipate the prospect of utilizing this transgenic *Daphnia* for studying the function and roles of HDR in asexual reproduction by manipulating the components of HDR machinery. The result would contribute to a further understanding of evolutionary genomics (Figure 21, manipulated components).

The HDR efficiency reported in mammals and plants is lower compared to NHEJ (Mao et al., 2008),(Mao et al., 2010) (Puchta, 2005) because it takes a longer time to complete than NHEJ (Mao et al., 2008) and functions only during S and G2 phases when the sister chromatid, the main template to repair DSB, is present (Pardo et al., 2009). Thus, several approaches have been developed to enhance genome editing by HDR such as inhibiting (Chu et al., 2015) or knocking out the key factor of NHEJ (Nakanishi et al., 2015), synchronizing and capturing cells at certain phases (S. Lin et al., 2014), and modifying the Cas9 by fusing it with a key protein necessary in the HDR steps (Charpentier et al., 2018). To evaluate the effects of these approaches on the HDR activity, the reporter system for visualizing the HDR event has been

used in mammalian cells (Słabicki et al., 2010). We suggest the potential use of DR-GFP *Daphnia* for optimizing HDR efficiency for instance by impairing the NHEJ repair genes (*Ku70* or *Lig4*) (Figure 21. manipulated components).

I also acknowledge the limitations of this reporter system. First, in live imaging, it may be difficult to detect the eGFP signals from mutated cells that are located deep inside the tissues, which may lower sensitivity for detecting eGFP positive cells and their quantification. This limitation could be addressed by sorting and counting the eGFP-positive cells using fluorescence-activated cell sorting (FACS). Second, the DR-GFP reporter system can only visualize the presence of HDR events at the reporter locus. This situation may affect the sensitivity for detection of the HDR triggered by environmental genotoxicants or mutagenic agents that may introduce random DSB throughout the genome. Therefore, other approaches to globally visualize HDR events in *Daphnia* may be developed. For instance, fusing the Förster resonance energy transfer (FRET) system in HDR key proteins to provide spatiotemporal visualization of their function (Gibbs et al., 2019). Third, for a comprehensive understanding of the DNA repair mechanism in this species, reporters for detection of the other DNA repair pathways such as NHEJ and SSA need to be developed. This limitation can be addressed by utilizing other reporter systems, such as “traffic light”, a dual fluorescence-based reporter which can visualize HDR and NHEJ repair pathways (Certo, et al. 2018). However, despite these possible limitations, DR-GFP reporter *Daphnia* would offer a valuable tool for the evaluation of HDR in this ecologically important species.

3.2 Conclusion

In this study, 1) I successfully integrated the DR-GFP system into *D. magna* genome and visualized HDR occurrence *in vivo*. 2) I evaluated the functionality of this reporter system by introducing targeted DSB in the reporter site. The observed eGFP signal and detected PCR products from the repaired eGFP gene in the injected daphniids, demonstrate evidence of

detection of HDR *in situ* based on the eGFP fluorescence. 3) I could also detect the repaired eGFP by qPCR. With some improvements, this method is potentially used for quantitative measurement of the HDR level following DNA DSB occurrences in the future. Furthermore, ubiquitous expression of mCherry that is bicistronically expressed with the DR-GFP suggests that this reporter system enables us to detect the HDR event in most types of cells.

REFERENCES

Adhitama, N., Matsuura, T., Kato, Y., & Watanabe, H. (2018). Monitoring ecdysteroid activities using genetically encoded reporter gene in *Daphnia magna*. *Marine Environmental Research*, **140**, 375-381

Aguilera, A., & Gómez-González, B. (2008). Genome instability: A mechanistic view of its causes and consequences. *Nature Reviews Genetics*, *9*(3), 204–217. https://doi.org/10.1038/nrg2268

Allers, T., & Lichten, M. (2001). Differential timing and control of noncrossover and crossover recombination during meiosis. *Cell*, *106*(1), 47–57. https://doi.org/10.1016/S0092-8674(01)00416-0

Andersen, S. L., & Sekelsky, J. (2010). Meiotic versus mitotic recombination: Two different routes for double-strand break repair. *BioEssays*, *32* (12), 1058–1066. https://doi.org/10.1002/bies.201000087

Arao, T., Kato, Y., Nong, Q. D., Yamamoto, H., Watanabe, H., Matsuura, T., Watanabe, H. (2020). Production of genome-edited *Daphnia* for heavy metal detection by fluorescence. *Scientific Reports*, *10*(1), 1–10. https://doi.org/10.1038/s41598-020-78572-z

Bekker, E. I., Karabanov, D. P., Galimov, Y. R., Haag, C. R., Neretina, T. V., & Kotov, A. A. (2018). Phylogeography of *Daphnia magna* Straus (Crustacea: Cladocera) in Northern Eurasia: Evidence for a deep longitudinal split between mitochondrial lineages. *PLoS ONE*, *13*(3), 1–20.

Bunting, S. F., Callén, E., Wong, N., Chen, H. T., Polato, F., Gunn, A., Nussenzweig, A. (2010). 53BP1 inhibits homologous recombination in brca1-deficient cells by blocking resection of DNA breaks. *Cell*, *141*(2), 243–254. https://doi.org/10.1016/j.cell.2010.03.012

Certo, Michael T.Byoung Y.Ryu , James E. Annis, Mikhail Garibov, Jordan V. Jarjour, David J. Rawlings, A. M. S. (2018). Tracking genome engineering outcome at individual DNA

breakpoints. *Nat Methods*, *8*(8), 671–676. https://doi.org/10.1038/nmeth.1648.Tracking

Charpentier, M., Khedher, A. H. Y., Menoret, S., Brion, A., Lamribet, K., Dardillac, E., Concordet, J. P. (2018). CtIP fusion to Cas9 enhances transgene integration by homology-dependent repair. *Nature Communications*, *9*(1), 1–11. https://doi.org/10.1038/s41467-018-03475-7

Chu, V. T., Weber, T., Wefers, B., Wurst, W., Sander, S., Rajewsky, K., & Kühn, R. (2015). Increasing the efficiency of homology-directed repair for CRISPR-Cas9-induced precise gene editing in mammalian cells. *Nature Biotechnology*, *33*(5), 543–548. https://doi.org/10.1038/nbt.3198

Colbourne, J. K., Pfrender, M. E., Gilbert, D., Thomas, W. K., Tucker, A., Oakley, T. H., Boore, J. L. (2011a). The ecoresponsive genome of *Daphnia pulex*. *Science*, *331*(6017), 555–561. https://doi.org/10.1126/science.1197761

Deininger, P. L., Morales, M. E., Ortego, J. C., Stark, J., Ade, C. M., Roy-Engel, A. M., & Derbes, R. S. (2016). Heavy Metal Exposure Influences Double Strand Break DNA Repair Outcomes. *Plos One*, *11*(3), e0151367. https://doi.org/10.1371/journal.pone.0151367

Donoho, G., Jasin, M., & Berg, P. (1998). Analysis of Gene Targeting and Intrachromosomal Homologous Recombination Stimulated by Genomic Double-Strand Breaks in Mouse Embryonic Stem Cells. *Molecular and Cellular Biology*, *18*(7), 4070–4078. https://doi.org/10.1128/mcb.18.7.4070

Forootan, A., Sjöback, R., Björkman, J., Sjögreen, B., Linz, L., & Kubista, M. (2017). Methods to determine limit of detection and limit of quantification in quantitative real-time PCR (qPCR). *Biomolecular Detection and Quantification*, *12*(September 2016), 1–6. https://doi.org/10.1016/j.bdq.2017.04.001

Gagnon, J. A., Valen, E., Thyme, S. B., Huang, P., Ahkmetova, L., Pauli, A., Schier, A. F.

(2014). Efficient Mutagenesis by Cas9 Protein-Mediated Oligonucleotide Insertion and Large-Scale Assessment of Single-Guide RNAs. *Plos One*, *9*(5), 5–12. https://doi.org/10.1371/journal.pone.0098186

Gibbs, D. R., & Dhakal, S. (2019). Homologous recombination under the single-molecule fluorescence microscope. *International Journal of Molecular Sciences*, *20*(23), 1–16. https://doi.org/10.3390/ijms20236102

Her, J., & Bunting, S. F. (2018). How cells ensure correct repair of DNA double-strand breaks. *Journal of Biological Chemistry*, *293*(27), 10502–10511. https://doi.org/10.1074/jbc.TM118.000371

Herbert, P. D. N. (1978). The Population Biology of Daphnia (Crustacea, Daphnidae). *Biological Review, 53, 387-426*, *53*, 387–426.

Honda, Y., Tsuchiya, K., Sumiyoshi, E., Haruta, N., & Sugimoto, A. (2017). Tubulin isotype substitution revealed that isotype combination modulates microtubule dynamics in *C. elegans* embryos. *Journal of Cell Science*, *130*(9), 1652–1661. https://doi.org/10.1242/jcs.200923

Huertas, P. (2010). DNA resection in eukaryotes : deciding how to fix the break. *Nat Struct Mol Biol.*, *17*(1), 11–16. https://doi.org/10.1038/nsmb.1710.DNA

Izzatur, N., Ismail, B., Kato, Y., Matsuura, T., & Id, H. W. (2018). Generation of white-eyed *Daphnia magna* mutants lacking scarlet function. *Plos One*, *11*, 1–11.

Johnson, N. M., Lemmens, B. B. L. G., & Tijsterman, M. (2013). A Role for the Malignant Brain Tumour (MBT) Domain Protein LIN-61 in DNA Double-Strand Break Repair by Homologous Recombination. *PLoS Genetics*, *9*(3), e1003339. https://doi.org/10.1371/journal.pgen.1003339

Kass, E. M., Helgadottir, H. R., Chen, C., Barbera, M., & Wang, R. (2013). Double-strand break repair by homologous recombination in primary mouse somatic cells requires

BRCA1 but not the ATM kinase. *Proceedings of the National Academy of Sciences*, *110*(March), 5564–5569. https://doi.org/10.1073/pnas.1216824110

Kato, Y., Matsuura, T., & Watanabe, H. (2012). Genomic Integration and Germline Transmission of Plasmid Injected into Crustacean *Daphnia magn*a Eggs. *PLoS ONE*, *7*(9), 0–6. https://doi.org/10.1371/journal.pone.0045318

Kato, Y., Perez, C. A. G., Mohamad Ishak, N. S., Nong, Q. D., Sudo, Y., Matsuura, T., Watanabe, H. (2018). A 5′ UTR-Overlapping LncRNA Activates the Male-Determining Gene doublesex1 in the Crustacean *Daphnia magna. Current Biology*, *28*(11), 1811-1817.e4. https://doi.org/10.1016/j.cub.2018.04.029

Kato, Y., Shiga, Y., Kobayashi, K., Tokishita, S. I., Yamagata, H., Iguchi, T., & Watanabe, H. (2011). Development of an RNA interference method in the cladoceran crustacean *Daphnia magna. Development Genes and Evolution*, *220*(11–12), 337–345. https://doi.org/10.1007/s00427-011-0353-9

Klüttgen, B., Dülmer, U., Engels, M., & Ratte, H. T. (1994). ADaM, an artificial freshwater for the culture of zooplankton. *Water Research*, *28*(3), 743–746. https://doi.org/10.1016/0043-1354(94)90157-0

Kumagai, H., Matsuura, T., Kato, Y., & Watanabe, H. (2017). Development of a bicistronic expression system in the branchiopod crustacean *Daphnia magna*. *Genesis*, *55*(12), 1–6. https://doi.org/10.1002/dvg.23083

Kumagai, H., Nakanishi, T., Matsuura, T., Kato, Y., & Watanabe, H. (2017). CRISPR/Cas-mediated knock-in via nonhomologous end-joining in the crustacean *Daphnia magna*. *PLoS ONE*, *12*(10), 1–12. https://doi.org/10.1371/journal.pone.0186112

Li, X., & Heyer, W. D. (2008). Homologous recombination in DNA repair and DNA damage tolerance. *Cell Research*, *18*(1), 99–113. https://doi.org/10.1038/cr.2008.1

Lin, F. L., Sperle, K., & Sternberg, N. (1984). Model for homologous recombination during

transfer of DNA into mouse L cells: role for DNA ends in the recombination process. *Molecular and Cellular Biology*, *4*(6), 1020–1034. https://doi.org/10.1128/mcb.4.6.1020

Lin, S., Staahl, B. T., Alla, R. K., & Doudna, J. A. (2014). Enhanced homology-directed human genome engineering by controlled timing of CRISPR/Cas9 delivery. *ELife*, *3*, 1–13. https://doi.org/10.7554/eLife.04766

Mao, Zhiyong, Michael Bozzella, Andrei Seluanov, and V. G. (2010). DNA repair by nonhomologous end joining and homologous recombination during cell cycle in human cells. *International Journal of Biochemistry and Molecular Biology*, *1*(1), 1–11.

Mao, Z., Bozzella, M., Seluanov, A., & Gorbunova, V. (2008). Comparison of nonhomologous end joining and homologous recombination in human cells. *DNA Repair*, *7*(10), 1765–1771. https://doi.org/10.1016/j.dnarep.2008.06.018

McGinnis, W., & Krumlauf, R. (1992). Homeobox genes and axial patterning. *Cell*, *68*(2), 283–302. https://doi.org/10.1016/0092-8674(92)90471-N

Morrow, D. M., Connelly, C., & Hieter, P. (1997). "Break copy" duplication: A model for chromosome fragment formation in saccharomyces cerevisiae. *Genetics*, *147*(2), 371–382. https://doi.org/10.1093/genetics/147.2.371

Nakanishi, T., Kato, Y., Matsuura, T., & Watanabe, H. (2014). CRISPR/Cas-mediated targeted mutagenesis in *Daphnia magna*. *PLoS ONE*, *9*(5), 1–7. https://doi.org/10.1371/journal.pone.0098363

Nakanishi, T., Kato, Y., Matsuura, T., & Watanabe, H. (2015). TALEN-mediated homologous recombination in *Daphnia magna*. *Scientific Reports*, *5*, 1–10. https://doi.org/10.1038/srep18312

Nakanishi, T., Kato, Y., Matsuura, T., & Watanabe, H. (2016). TALEN-mediated knock-in via non-homologous end joining in the crustacean *Daphnia magna*. *Scientific Reports*, *6*(November), 1–7. https://doi.org/10.1038/srep36252

OECD. (2004). Test No. 202: *Daphnia* sp. acute immobilisation test. *OECD Guidelines for Testing of Chemicals*. https://doi.org/10.1016/0006-8993(75)90486-2

OECD. (2012). Test guideline No. 211: Daphnia magna reproduction test. *OECD Guidelines for the Testing of Chemicals*, (211).

Osaki, J. H., Espinha, G., Magalhaes, Y. T., & Forti, F. L. (2016). Modulation of RhoA GTPase Activity Sensitizes Human Cervix Carcinoma Cells to γ-Radiation by Attenuating DNA Repair Pathways. *Oxidative Medicine and Cellular Longevity*, *2016*. https://doi.org/10.1155/2016/6012642

Paix, A., Folkmann, A., Goldman, D. H., Kulaga, H., Grzelak, M. J., Rasoloson, D., Seydoux, G. (2017). Precision genome editing using synthesis-dependent repair of Cas9-induced DNA breaks. *Proceedings of the National Academy of Sciences of the United States of America*, *114*(50), E10745–E10754. https://doi.org/10.1073/pnas.1711979114

Paliwal, S., Kanagaraj, R., Sturzenegger, A., Burdova, K., & Janscak, P. (2014). Human RECQ5 helicase promotes repair of DNA double-strand breaks by synthesis-dependent strand annealing. *Nucleic Acids Research*, *42*(4), 2380–2390. https://doi.org/10.1093/nar/gkt1263

Panganiban, G., & Rubenstein, J. L. R. (2002). Developmental functions of the Distal-less/Dlx homeobox genes. *Development*, *129*(19), 4371–4386. https://doi.org/10.1242/dev.129.19.4371

Pardo, B., Gómez-González, B., & Aguilera, A. (2009). DNA double-strand break repair: How to fix a broken relationship. *Cellular and Molecular Life Sciences*, *66*(6), 1039–1056. https://doi.org/10.1007/s00018-009-8740-3

Pierce, A. J., Johnson, R. D., Thompson, L. H., & Jasin, M. (1999a). XRCC3 promotes homology-directed repair of DNA damage in mammalian cells. *Genes and Development*, *13*(20), 2633–2638. https://doi.org/10.1101/gad.13.20.2633

Pierce, A. J., Johnson, R. D., Thompson, L. H., & Jasin, M. (1999b). XRCC3 promotes homology-directed repair of DNA damage in mammalian cells service. *Genes and Development*, *13*, 2633–2638.

Puchta, H. (2005). The repair of double-strand breaks in plants: Mechanisms and consequences for genome evolution. *Journal of Experimental Botany*, *56*(409), 1–14. https://doi.org/10.1093/jxb/eri025

Ran, F. A., Cong, L., Yan, W. X., Scott, D. A., Gootenberg, J. S., Kriz, A. J., Zhang, F. (2015). In vivo genome editing using Staphylococcus aureus Cas9. *Nature*, *520*(7546), 186–191. https://doi.org/10.1038/nature14299

Ryan, M. D., King, A. M. Q., & Thomas, G. P. (1991). Cleavage of foot-and-mouth disease virus polyprotein is mediated by residues located within a 19 amino acid sequence. *Journal of General Virology*, *72*(11), 2727–2732. https://doi.org/10.1099/0022-1317-72-11-2727

Schmidt, M. J., Gupta, A., Bednarski, C., Gehrig-Giannini, S., Richter, F., Pitzler, C., Coco, W. M. (2021). Improved CRISPR genome editing using small highly active and specific engineered RNA-guided nucleases. *Nature Communications*, *12*(1). https://doi.org/10.1038/s41467-021-24454-5

Seluanov, A., Mao, Z., & Gorbunova, V. (2010). Analysis of DNA Double-strand Break (DSB) Repair in Mammalian Cells. *Journal of Visualized Experiments*, (43), 1–6. https://doi.org/10.3791/2002

Shahar, O. D., Kalousi, A., Eini, L., Fisher, B., Weiss, A., Darr, J., Soutoglou, E. (2014). A high-throughput chemical screen with FDA approved drugs reveals that the antihypertensive drug Spironolactone impairs cancer cell survival by inhibiting homology directed repair. *Nucleic Acids Research*, *42*(9), 5689–5701. https://doi.org/10.1093/nar/gku217

Słabicki, M., Theis, M., Krastev, D. B., Samsonov, S., Mundwiller, E., Junqueira, M., Buchholz, F. (2010). A genome-scale DNA repair RNAi screen identifies SPG48 as a novel gene associated with hereditary spastic paraplegia. *PLoS Biology*, *8*(6), e1000408. https://doi.org/10.1371/journal.pbio.1000408

Stark, J. M., Pierce, A. J., Oh, J., Pastink, A., & Jasin, M. (2004). Genetic Steps of Mammalian Homologous Repair with Distinct Mutagenic Consequences. *Molecular and Cellular Biology*, *24*(21), 9305–9316. https://doi.org/10.1128/MCB.24.21.9305-9316.2004

Szostak, J. W., Orr-Weaver, T. L., Rothstein, R. J., & Stahl, F. W. (1983). The double-strand-break repair model for recombination. *Cell*, *33*(1), 25–35. https://doi.org/10.1016/0092-8674(83)90331-8

Törner, K., Nakanishi, T., Matsuura, T., Kato, Y., & Watanabe, H. (2018). Genomic integration and ligand-dependent activation of the human estrogen receptor α in the crustacean Daphnia magna. *PLoS ONE*, *13*(6), 1–11. https://doi.org/10.1371/journal.pone.0198023

Vriend, L. E. M., Jasin, M., & Krawczyk, P. M. (2014). *Assaying break and nick-induced homologous recombination in mammalian cells using the DR-GFP reporter and cas9 nucleases*. *Methods in Enzymology* (1st ed., Vol. 546). Elsevier Inc. https://doi.org/10.1016/B978-0-12-801185-0.00009-X

Yeh, C. D., Richardson, C. D., & Corn, J. E. (2019). Advances in genome editing through control of DNA repair pathways. *Nature Cell Biology*, *21*(12), 1468–1478. https://doi.org/10.1038/s41556-019-0425-z

Acknowledgements

I would like to express my sincere gratitude to my supervisor Professor Dr. Hajime Watanabe for giving me the great opportunity to pursue my master and doctoral degree as a member of Bioenvironmental Science Laboratory under his guidance. To Associate Professor Dr. Yasuhiko Kato for his guidance in every step of my research and for patiently teaching me to be a good scientist.

I would also like to extend my gratitude to Professor Toshiya Muranaka from Department of Biotechnology and Professor Kohsuke Honda from the International Center for Biotechnology, Graduate School of Engineering, Osaka University, for their valuable comments and suggestion during the dissertation writing and final presentation.

I also acknowledge the Department of Biotechnology, Osaka University, and Monbukagakusho Scholarship (MEXT) for the financial support.

I would like to thank the staff and lab members of Watanabe Laboratory for their great help and friendship for this past 5 years.

Finally, from the bottom of my heart I would like to thank my husband (and my Assistant Professor Dr. Nikko Adhitama); my lovely daughter, Kayla Fathia Adhitama; and my parents in Indonesia for being the source of my strength to finish this PhD journey.